SYNERGISTIC ACTION OF RNA POLYMERASE IN OVERCOMING THE NUCLEOSOMAL BARRIER

A Dissertation

Presented to the Faculty of the Graduate

of Cornell University

In Partial Fulfillment of the Requirements for the Degree of

Doctor of Philosophy

by

Jing Jin

August 2009

SYNERGISTIC ACTION OF RNA POLYMERASE IN OVERCOMING THE NUCLEOSOMAL BARRIER

Jing Jin, Ph. D.

Cornell University 2009

During gene expression, RNA polymerase (RNAP) encounters a major barrier at a nucleosome and yet it must access the nucleosomal DNA. It has been proposed that multiple RNAPs might increase transcription efficiency through nucleosomal DNA. Here we have quantitatively investigated this hypothesis by using *E. coli* RNAP as a model system and directly monitoring its location on the DNA via a single molecule DNA unzipping technique. When a single RNAP encountered a nucleosome, it paused with a distinctive 10-bp periodicity and was backtracked by an average distance of ~10-15 bp. When two RNAPs were elongating in close proximity, the trailing RNAP exerted an assisting force on the leading RNAP, reducing its backtracking and enhancing its transcription through a nucleosome ~5-fold. Taken together, our data indicate that histone-DNA interactions within a nucleosome dictate RNAP pausing behavior, and that alleviation of nucleosome-induced backtracking by multiple polymerases is a likely mechanism for overcoming the nucleosomal barrier in vivo.

BIOGRAPHICAL SKETCH

Jing Jin was born July 1st, 1980 in Nanjing, China. While growing up in Nanjing JieFangLu elementary school and Nanjing No.34 Middle School, she luckily received three years education in Nanjing High School Attached to Nanjing Normal University, which is considered as a very best high school in the city of Nanjing. She later was accepted in physics department, Nanjing University in 1998, where she had her four years intensive training as a physicist. Nanjing University created a healthy environment to encourage students to purser higher education, benefited from which, she continued her graduate studies in Cornell University, USA, where she was exposed to a new field, biophysics and got interested. In the summer of 2003, she began graduate researches in Michelle Wang's laboratory at Cornell University, Department of Physics. Her major project was to study RNA polymerase transcription process while elongating through a nucleosome. She received her Ph.D. in August, 2009 in the subject of Physics and the field of Biophysics.

To my family and friends

ACKNOWLEDGMENTS

First of all, I would like to give many thanks to my advisor, Michelle Wang, who has been not only a scientific supervisor to me, but also a friendly mentor. I appreciate that when I was immature and inexperienced in research during my early graduate studies, she presented extreme patience and encouragement to me. She guided me gradually to the right track and trained me to be an independent thinker. I enjoyed intensive working with her when we prepared my paper together. Her personality has strongly influenced me and she demonstrated me the essential qualities as a good scientist: hard working, persistence and rigorousness. Dr. Wang cares for me beyond my laboratory work, she concerns about me when I have my personal issues. She has always been a good person to talk to, to seek advice from.

I also appreciate the support of my other special committee members, Professors James Sethna and Lee Kraus, who have provided guidance throughout my time in graduate school. In addition, I am thankful to Professor Mikhail Kashlev, our collaborator, who provided precious opportunity for me to learn skills in NIH as well as contributed to finalize my paper.

I am grateful that I have been working with a team of creative and friendly labmates, who helped me with my experimental difficulties, had valuable suggestions to my day to day research. I want to give special thanks to Lucy Bai, who taught me bench work skills hand by hand, had constructive discussions with me throughout my graduate life. Daniel Johnson, who sat

next to me, had encouraged me when I was in my troughs. Scott, Chris, Ben, Maxim, thank you all for constant support and inspiring suggestions.

I am very lucky to know many friends during the time I studied in Cornell. Miao Wang, whom I got to know from the first day I arrived at Cornell. Since then, we have been extremely good to each other. We helped each other during course studies, personal confusions. We shared happiness and frustrations. Hui Chen, who graduated from the same college as me, helped me going through my personal difficulties. I enjoyed time with her talking and shopping. John Read, Curry Tayor, I am happy to be in the same year with you guys, and have you to fight hard together with me during my graduate life. It's hard to list all of their names; I wish them the best and have a beautiful future.

In the end, I would like to mention my most beloved family, my parents and my husband. My parents provided me good educations and encouraged me to pursue my dreams. Although taking my graduate study in the USA means leaving them thousands and thousands miles away, although they miss me every moment, they have been unconditionally supportive. My husband, Yong, you must know how much grateful I am to be with you. You truly care about me, help me with my life and my career. You are the best thing ever happened to me, and I am happy I made great progress after we are together. I want to dedicate this dissertation to all of you, my family and my friends. Without you, I will not be who I am now.

TABLE OF CONTENTS

LIST OF FIGURES

LIST OF TABLES

CHAPTER ONE:
OVERVIEW OF RNA POLYMERASE TRANSCRIPTION THROUGH MONONUCLEOSOME

BACKGROUND OF RNA POLYMERASE TRANSCRIPTION

Transcription is the key step in gene expression and regulation. During transcription, DNA-dependent RNA polymerase (RNAP) (*E.coli* RNAP in bacteria and RNA polymerase II (Pol II) in eukaryotes) translocates unidirectionally along the DNA double helix and faithfully copies its genetic information stored in the DNA nucleic acid sequences into a complementary RNA strand, called message RNA (mRNA), by addition of ribonucleotide triphosphates (rNTPs) units to the mRNA's 3'-hydroxyl end using a 5' to 3' fashion. mRNA is further decoded by ribosome and is translated into protein.

Bacterial RNA Polymerase and Eukaryotic RNA Polymerases

"Multisubunit RNAP family" contains RNAPs from bacteria, archaea, and eukaryotes. Although evolutionarily distant, the structures of the RNAPs in these organisms are amazingly conserved (Table 1.1). As illustrated by the structure of the core RNAP in bacteria T. aquaticus (Figure 1.1), it has the shape reminiscent of a crab claw, with two pincers (composed of β and β' subunits) defining an internal channel which is large enough to accommodate ds DNA and RNA/DNA hybrid. α^{I} and α^{II} are of the identical sequence and located on the other side of the channel (Zhang et al., 1999). Besides the internal channel, each RNAP also contains a NTP entry channel (or secondary channel) and an RNA exit channel. Mg^{2+} is required for RNAP activity. One Mg^{2+} is tightly bound with the active site which is located in the junction of the internal channel and the secondary channels.

Table 1.1. Conserved Subunits of Bacterial RNAP, Archaeal RNAP, Eukaryotic RNAP I, II, and III.

Molecular Weight	Bacterial RNAP	Eukaryotic Pol II	Eukaryotic Pol I	Eukaryotic Pol III	Archaeal RNAP
~ 160 kDa	β'	RPB1	RPA1	RPC1	A'/A"
~ 150 kDa	β	RPB2	RPA2	RPC2	B
~ 35 kDa	α^{I}	RPB3	RPC5	RPC5	D
~ 10-35 kDa	α^{II}	RPB11	RPC9	RPC9	L
~ 6 kDa	ω	RPB6	RPB6	RPB6	K
		+ 7 others	+ 9 others	+ 11 others	+ 6 others

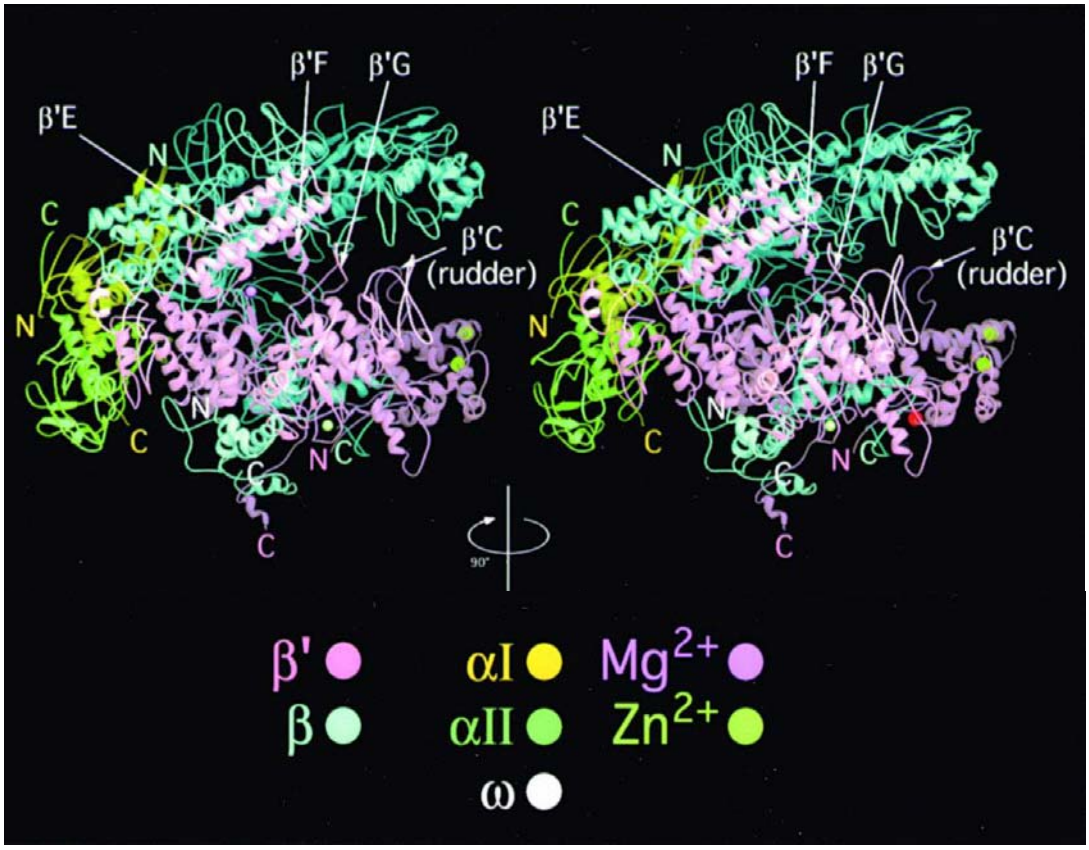

Figure 1.1. Structure of T. aquaticus Core RNAP (adapted from Zhang et al., 1999)

The molecule is 150 Å X 115 Å X 110 Å. The shape is reminiscent of a crab claw, with two pincers primarily made of β and β' subunits.

The high degree of structural conservation makes *E. coli* RNAP a good model system to study eukaryotic Pol II transcription properties, especially that *E.coli* RNAP requires no transcription factors for transcription initiation which greatly simplifies the model system. In addition, *E. coli* RNAP has been found to exhibit very similar behavior as yeast Pol II regarding its transcription mechanism in vitro (Walter et al., 2003). For instance, yeast Pol II and *E.coli* RNAP are both responsible for transcribing mRNA. Backtracking has been observed for both RNAPs (Komissarova and Kashlev, 1997; Toulme et al., 2000; Shaevitz et al., 2003). Furthermore, when encountering a major barrier at a nucleosome, *E.coli* RNAP pauses at essentially identical sites to those of Pol II at a nucleosome (Walter et al., 2003). While *E.coli* RNAP and yeast Pol II share many similarities, they differ dramatically from yeast RNA polymerase III (Pol III). For instance, Pol III primarily transcribes tRNA and transcribes through a nucleosome much more readily (Studitsky et al., 1997). Pol III is not known to backtrack and the mechanism for its transcription through nucleosomes has been shown to be dramatically different from that of Pol II (Studitsky et al., 1997; Walter et al., 2003).

The Transcription Cycle

Transcription is a cyclic process that is traditionally divided into three major steps: initiation, elongation and termination. Initiation requires a specific DNA sequence (promoter region), which is normally found around -10 to -35 base pair (bp) upstream of the transcription start site. Prior to initiation, RNAP and various transcription factors form “closed complex”. Although most genes contain consensus sequence TATA box in their promoter region, different

promoter sequences could vary considerably, leading to the difference in their binding specificity, affinity and initiation efficiency of RNAPs. Upon forming the closed complex, RNAP melts the duplex DNA around the transcription start site to open a transcription bubble, generating the “open complex”. The exposed DNA serves as a transcription template. From there, RNAP undergoes abortive initiation, in which RNAP repeatedly generates, releases and resynthesizes short RNA transcripts.

Once the nascent RNA reaches a critical length, 9-11 nucleotides (nt), stable transcription elongation complex (TEC) forms, and RNAP escapes from the promoter and enters productive elongation phase. During elongation, individual ribonucleotide is sequentially added to the 3’ end of RNA based on the DNA sequence. It is worth noting that since DNA is a helix, the elongation along DNA requires the rotation motion of RNAP relative to DNA. However, DNA strand rotation is often restricted by DNA-binding proteins and other structural barriers. Therefore, RNAP elongation results in positive supercoils in front and negative supercoils behind. Elongation is not a uniform process, each nucleotide addition competes with various transcription off-pathways which are considered to have regulatory importance (Figure 1.2). For instance, pausing (transient entry of inactive state) and arrest (complete halting without dissociation) may associate with proof reading, allowing timely interaction of regulatory factors (Greive and von Hippel, 2005). Backtracking (RNAP slides backwards and relocates its 3’ end away from active center) is thought to occur during transcription-coupled repair so that the lesion site is exposed to the repair specific proteins (Woudstra et al., 2002). Termination is triggered by specific sequence coded for a termination hairpin in the RNA followed by a U-

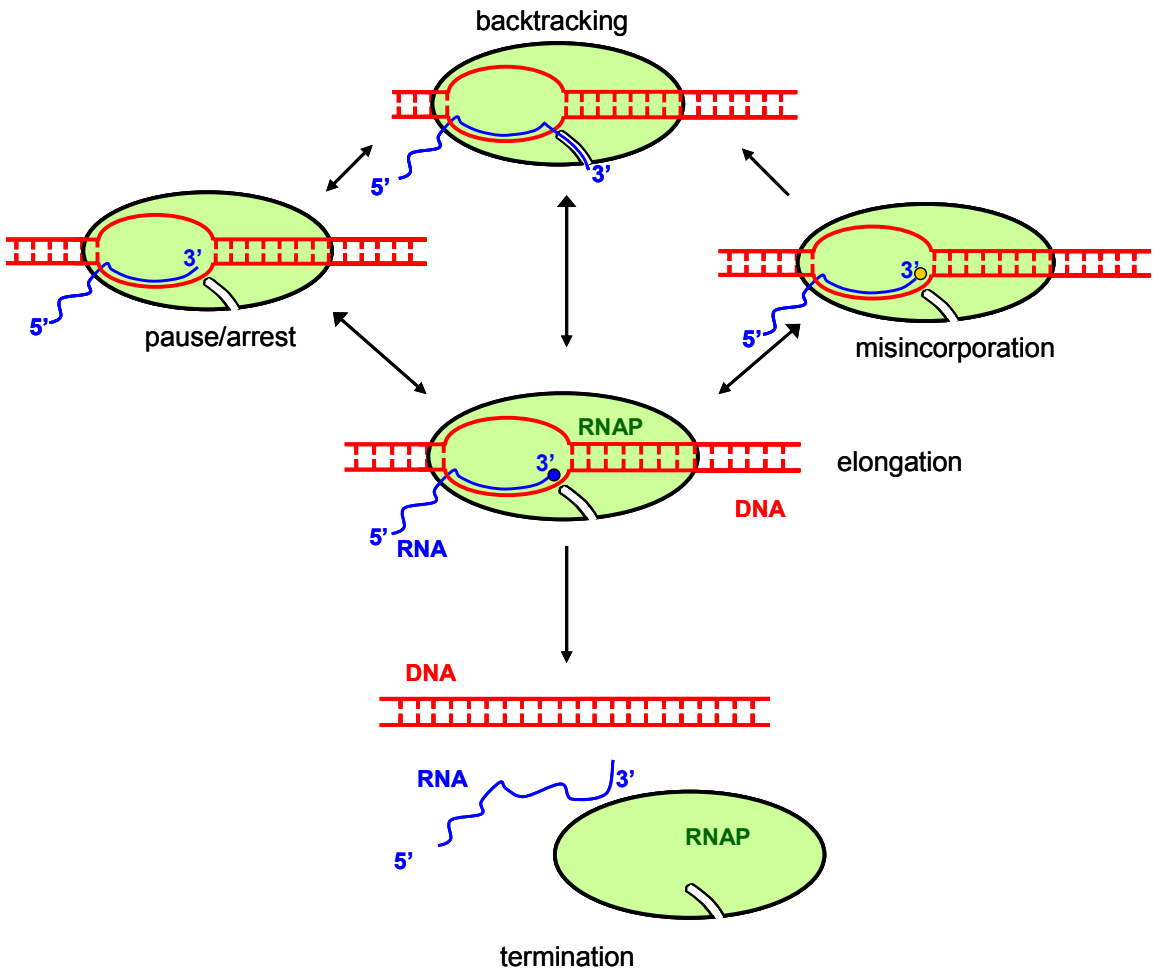

Figure 1.2. Schematic Illustration of Transcription Elongation Pathway

The productive elongation can branch off to several elongation off-pathways. Misincorporation-induced pauses are triggered by addition of a mismatch NTP (yellow dot) to the 3' end of RNA.

rich stretch, or the binding of the external factor ρ. Termination completes transcription cycle and allows RNAPs to be reused in the subsequent transcription processes.

Single Molecule Study on RNAP Transcription

Single Molecule techniques have made tremendous contributions in our understanding of transcription by RNAPs. These new approaches, including single-molecule fluorescence, atomic-force microscopy (AFM), magnetic tweezers and optical traps, offer many advantages in measuring kinetic and mechanical properties of molecules over conventional biochemical assays. First and most importantly, bulk measurements represent the average behavior of a large population which may obscure the difference among individual molecules. Secondly, some experimental designs using fluorescence energy transfer (FRET), magnetic tweezers and optical traps allow continuous measurement of a single molecule motion which fills in the gaps of the motion snapshots in biochemical studies and the transient intermediates are possible to obtain. Furthermore, single molecule techniques also provide tools to mechanical manipulate bio-molecules, such as exerting force and torque on DNA or proteins. Nevertheless, we also realize that the current single molecule techniques require a relative simple system which may not well represent the true environment for the bio-reactions. Also, the alteration of the system (fluorophore labeling, surface attachment of molecules, photodamage, etc.) may perturb the bio-molecule stability and bio-reaction pathways. Moreover, in order to get statistically meaningful results, large amount of data must be acquired and this can be time consuming. Despite of

the drawbacks, single molecules approaches provide diverse techniques which are suited for measuring different aspects of transcription. In the following paragraphs, I will discuss some important findings that have resulted from these techniques.

Historically, initiation process has drawn large attentions due to the two lines of seemingly controversial observation. Firstly, abortive initiation produces up to 8 nt RNA transcript; meanwhile, DNA-footprinting assay revealed that the upstream boundary of the DNA segment protected by RNAP remains unchanged during abortive initiation. Three putative mechanisms were proposed for how the RNAP active center translocates relative to DNA in initiation transcription (Figure 1.3a). The “scrunching” model argues that DNA can act as a flexible polymer; the additional unwound DNA can be pulled into RNAP to form single-stranded bulges. The “inchworm” model allows RNAP separation: the part containing the active center detaches from the rest of RNAP and translocates downstream. The “transient excursions” model assumes RNAP translocates forward and reverse as a unit but with rapid frequency, which results in an undetectable signal in time-averaged assays, such as DNA-footprinting. To differentiate among these three mechanisms, Strick lab utilized magnetic tweezers to torsionally constrain a single DNA template (Revyakin et al., 2006). Linking number conservation law states that the unwinding of one turn of promoter DNA by RNAP will result in a compensation gain of one positive supercoil or loss of one negative supercoil. The large change in the DNA tether length due to the change of numbers of supercoils provides 1 bp spatial resolution (Figure 1.3b). Among three models, only the “scrunching model” involves DNA unwinding, therefore, the observed

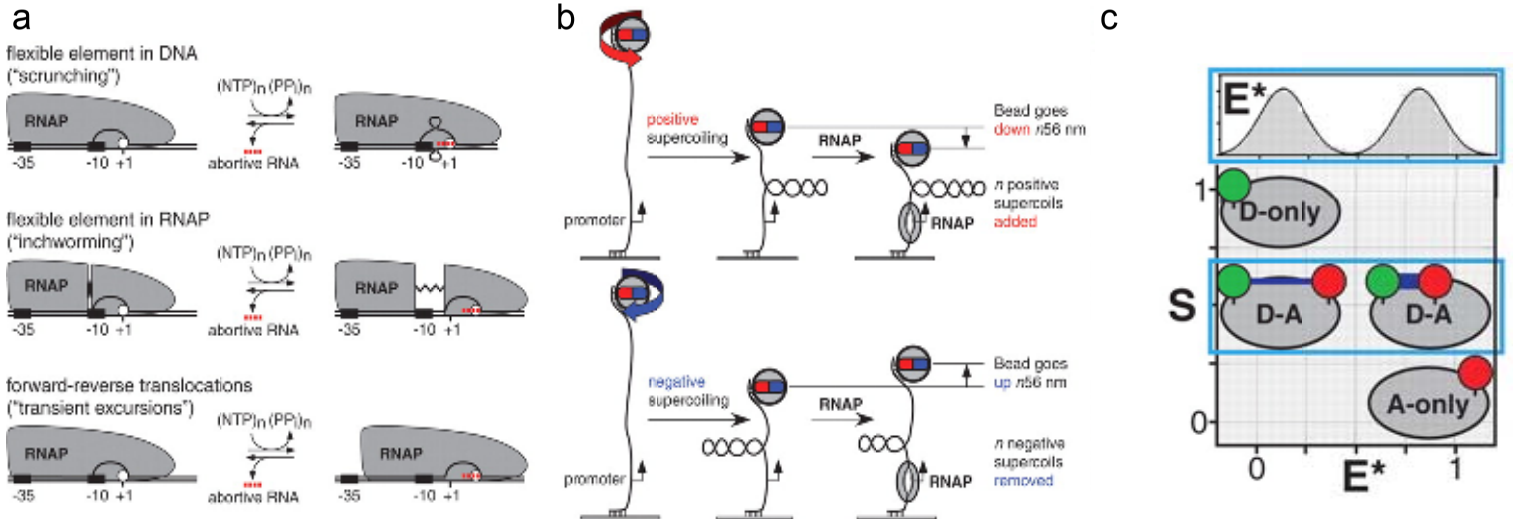

Figure 1.3. Single Molecule Study to Differentiate Three Putative Mechanisms of Initiation Transcription

(a) Three models have been proposed for RNAP active center translocation during Initiation (adapted from Revyakin et al., 2006). Scrunching, inchworming, and transient excursions. White circles, RNAP active center; red dotted line, RNA; black rectangles, promoter -10 and -35 elements.

(b) Magnetic tweezers were used to magnify the RNAP-dependent DNA unwinding signal. The unwinding of one turn of promoter DNA by RNAP will result in a compensation gain of one positive supercoil or loss of one negative supercoil (adapted from Revyakin et al., 2006).

(c) Illustration of FRET measurement of distances between donors (D) and acceptors (A). (adapted from Kapanidis et al., 2006).

DNA length fluctuations supported DNA scrunching. Independently, Ebright lab placed fluorescence donor and acceptor at different places of RNAP and DNA template, using FRET, they were able to determine whether there were any conformational alterations between the locations of donor and acceptor (Figure 1.3c). Their results also provided evidence for "scrunching model" as the primary mechanism for *E.coli* RNAP initiation (Kapanidis et al., 2006).

The application of single molecule techniques has provided several new insights into the nature of transcription elongation whose kinetics is hard to obtain by ensemble bulk measurements. The initial kinetic study of transcription elongation employed the tether particle motion (TPM) assay (Figure 1.4a) which observed the active elongation in single molecule level and measured the rates of *E.coli* RNAP elongation (Schafer et al., 1991; Yin et al., 1994). However, due to the large Brownian motion of the tethered bead, the on-path way could not be differentiated from the off-pathway. This problem was soon after resolved by introducing an external force applied by an optical trap to reduce the Brownian motion. The most commonly used experimental configuration is illustrated in Figure 1.4b. The variations include the use of dumbbell lasers (Figure 1.4c) or micropipette (Figure 1.4d). By following individual RNAP motion, researches have shown that transcription elongation is often interrupted by various pauses (Shundrovsky et al., 2004; Herbert et al., 2006); *E.coli* RNAP can continue against forces up to 20 pN (Wang et al., 1998), while Pol II is unable to transcribe under 8 pN force (Galburt et al., 2007); backtracking was directed observed (Wang et al., 1998; Galburt et al., 2007), and force-velocity relationship was characterized under different temperatures (Wang et al., 1998; Bai et al., 2007; Mejia et al., 2008).

Much effort has been made to increase the resolution via either noise reduction (Abbondanzieri et al., 2005; Moffitt et al., 2006) or introducing landmarks on the transcription sequences (Shundrovsky et al., 2004). Recently, Block and co-workers constructed an ultra-stable optical trapping system with angstrom-level resolution which allowed them to observe clear display of steps of 3.7 ± 0.6 Å on average under low NTP concentration (2.5-10 μM) and moderate loads (18 pN assisting force) (Abbondanzieri et al., 2005). The observation of the single-basepair stepping, together with the computational analysis, is inconsistent with previous proposed inchworming (RNAP is a flexible element, its upstream and downstream portion can move out of phase) and power stroke (pyrophosphate release drives motion) elongation models. Instead, it supports the Brownian ratchet model, in which RNAP can slide laterally on the DNA template due to thermal energy and the incorporation of the next nucleotide biases the polymerase forward by one base pair.

Termination occurs upon RNAP encountering an intrinsic termination sequence or being mediated by external factors ρ. ρ is thought to move along the nascent RNA until it reaches RNAP and signal the disassembly of the ternary complexes (Richardson and Richardson, 1996). Intrinsic termination sequence encodes an RNA sequence so that it can form a stable GC rich hairpin followed by a U-stretch (Lesnik et al., 2001; Nudler and Gottesman, 2002). The functions of hairpin and U-stretch in termination have been of great interest. The early TPM experiment has suggested that termination is an irreversible process because RNAP found to dwell before termination lacks the

Figure 1.4. Cartoon of Single Molecule Experimental Configurations Used in Elongation Studies

Laser beam: red; microspore: blue; DNA: red; RNAP: green; RNA: blue

(a) Tether particle motion. A DNA template is tethered by a small particle and an RNAP which is immobilized onto a microscope cover-glass surface. The range of the Brownian motion of the tethered particle is an indication of the DNA length.

(b) Optical trapping. The configuration is similar as in TPM. However, the small particle is held in an optical trap so that assisting or resisting force can be applied to the RNAP motion.

(c) Dumbbell optical trapping. Two beads, one is attached to one end of the DNA, the other is tagged with elongating RNAP, are suspended above the glass surface, which can eliminate the drift from microscopy stage.

(d) Micropipette assay. One bead, which is attached by elongating RNAP, is held by micropipette suction. Another free bead is attached to the distal end of the DNA. Fluid flow exerts forces on the free bead.

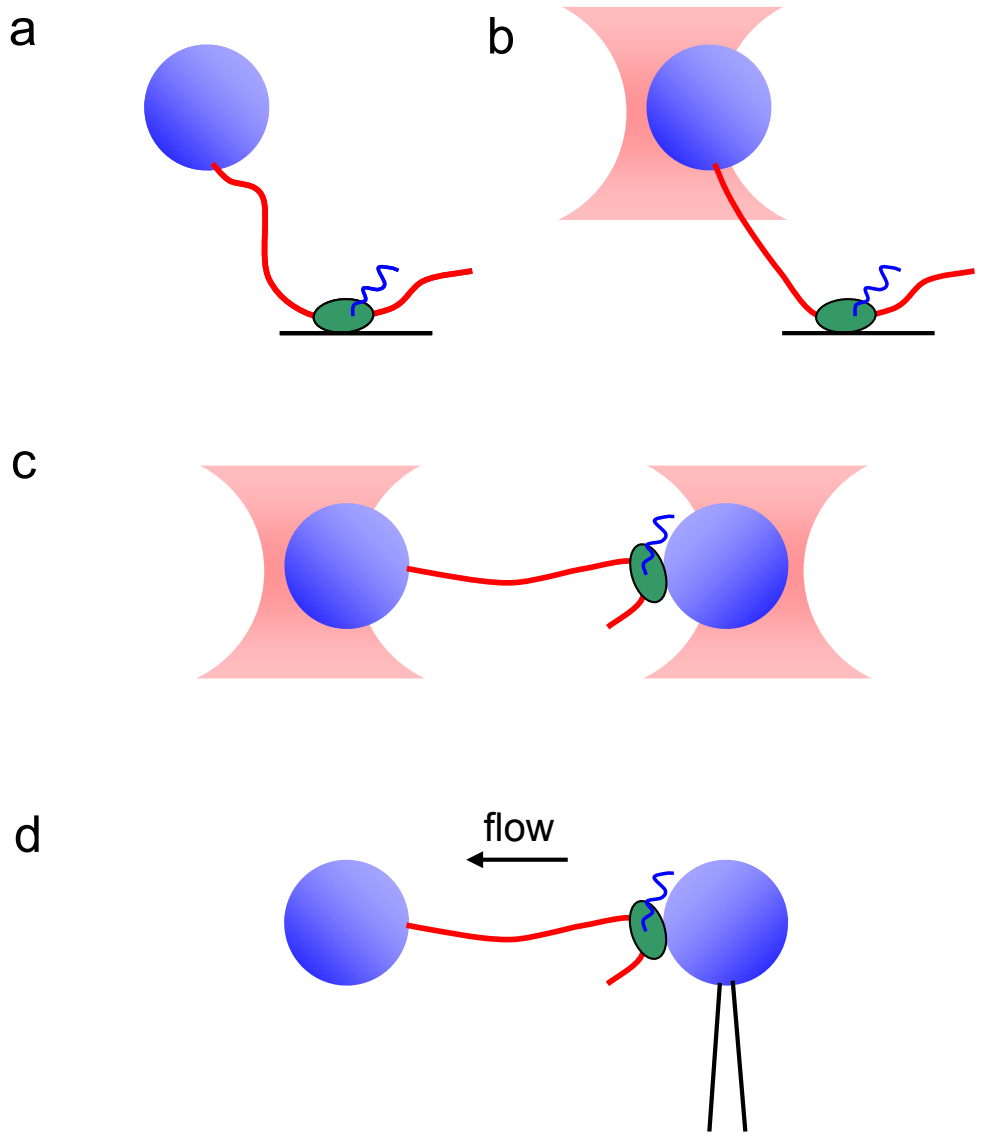
a
b
c
d
flow

corresponding pauses if termination site is successfully readthrough (Yin et al., 1999). However, this work was questioned due to the concern that the immobilization of RNAP would significantly reduce the DNA diffusion rate (Kashlev and Komissarova, 2002). A recently work from Block lab employed dumbbell experimental configuration to apply forces either between DNA strand and RNAP or RNAP and 5' RNA directly. They reinforced the argument that termination is a pathway energetically competing with active elongation. Termination efficiency is determined by the upstream secondary structure in RNA, termination hairpin and U-stretch after hairpin. Upon encountering a terminator sequence, if termination hairpin is not properly formed due to kinetic competition with the upstream secondary structure, RNAP reads through. Otherwise, termination occurs through alternative mechanisms of shearing or forward translocation. At t500 terminator, RNAP has to first forward translocate ~1.4 bp which induces terminal dwell, and the subsequent shearing of RNA and DNA template completes complex dissociation. At *his* and *tR2* terminators, RNAP skips the forward translocation step, the shearing motion of the RNA:DNA hybrid results in RNAP termination (Larson et al., 2008).

BACKGROUND OF NUCLEOSOME AND NUCLEOSOME REMODELING

Nucleosome is the fundamental repeating subunit of eukaryotic chromatin. Histone octamer, which is composed of 2 copies of 4 different subunits: H2A, H2B, H3 and H4, wrapped by 146bp of DNA in 1.67 left-handed superhelical turns constitutes the nucleosome core particle. The presence of highly basic histone proteins neutralizes DNA negative charges, and thus allows rigid DNA polymer fold extensively into cell nucleus. Adjacent nucleosomes are interconnected through linker DNA, leading to the next level of the chromatin organization known as the nucleosomal array, which will further fold into a 30-40nm fiber in the presence of linker histones.

Nucleosomal DNA Accessibility through Nucleosome Dynamics and Nucleosome Remodeling

Nucleosomes are ubiquitously distributed on chromosomes in eukaryotic cells; they occupy genes, regulatory sequences, such as promoters. Therefore, how nucleosomes can be unwrapped so that the covered genomic information of nucleosomal DNA can be accessed is of great interest. The nucleosome has been shown to be a dynamic structure. The entry and exit of nucleosomal DNA undergoes rapid unwrapping and rewrapping breathing motion, facilitating the invasion of the nucleosome (Li and Widom, 2004). However, this result might be complicated by the photophysical properties of the acceptor dye in the FRET experiment. Further FRET study using reagent that suppresses photoblinking demonstrated that the breathing motion does occur

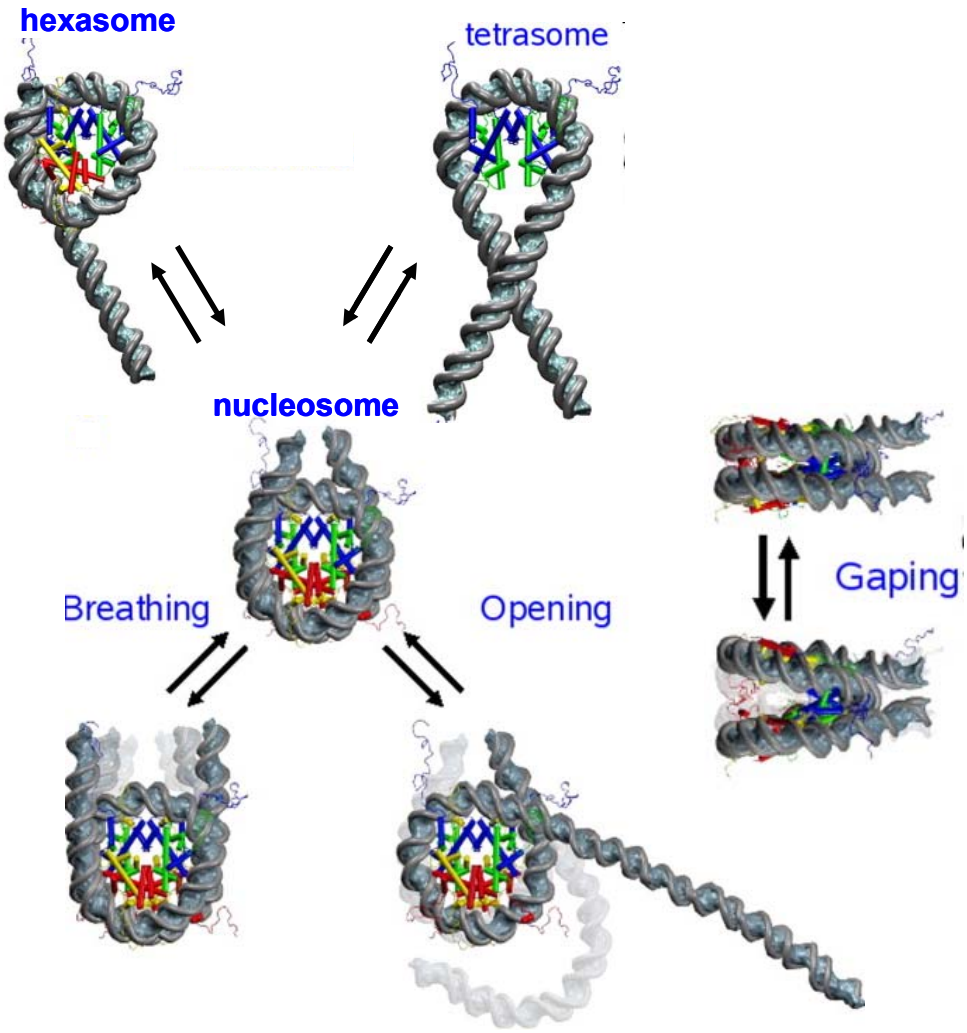

Figure 1.5. Nucleosome Dynamics

Nucleosome dynamics can be induced by breaking DNA/histone interactions and interchange of different forms of specific histone compositions. H2A, yellow; H2B, red; H3, blue; H4, green.

but with much less frequency. Long range opening was also observed (Rasnik et al., 2006; Tomschik et al., 2009). In addition, theoretical studies also predicted another kind of nucleosome dynamics, termed “gapping transition” (Mozziconacci and Victor, 2003), which involves breaking of histone/histone contacts (Figure 1.5). Furthermore, under thermally favorable conditions, nucleosomes can slide along the DNA sequence without disruption of histone octamer (Pennings et al., 1989).

In addition to the DNA/histone interaction-induced nucleosome dynamics, nucleosomes can also occur in different forms based on specific histone composition (Figure 1.5). Hexasomes, which lack one of the H2A/H2B dimers, have been found in both in vitro and in vivo experiments. H2A/H2B dimer undergoes rapid exchange during nucleosome remodeling process and transcription associated activities (Kimura and Cook, 2001; Kireeva et al., 2002; Bruno et al., 2003; Thiriet and Hayes, 2005). The temporal removal of H2A/H2B dimer facilitates transcription, meanwhile ensures the fast reform of the nucleosomes. Tetrasome is composed of only H3/H4 teramer, missing both H2A/H2B dimers. DNA in the tetrasome is wrapped in less than one superhelical turn (Alilat et al., 1999). A recent study reconstituted histone proteins onto a closed circular DNA. They showed that positive stress in the DNA is readily to dissociate one of the H2A/H2B dimer. And T7 RNAP elongation-induced stress stimulates the dissociation of the other H2A/H2B, leaving stable tetrasomes behind (Levchenko et al., 2005).

Although nucleosome intrinsic variability contributes to the accessibility of the nucleosomal DNA, nucleosome remodeling complexes play an important role

in exposing regulatory sites. Nucleosome remodeling complexes remodel nucleosomes via various mechanisms, including covalent modification of the histone tails (Brown et al., 2000; Anderson et al., 2001; Anderson and Widom, 2001), transient exposal of nucleosomal DNA by creating DNA loops on the nucleosome surface (Kassabov et al., 2003; Smith and Peterson, 2005; Zhang et al., 2006), translational reposition nucleosomes to uncover the regulatory sites (Whitehouse et al., 2003; Yang et al., 2006), nucleosome removal and redeposite (Belotserkovskaya et al., 2003; Koyama et al., 2004), and replacement of histone subunits (Kobor et al., 2004; Mizuguchi et al., 2004; Konev et al., 2007).

Single Molecule Study on Nucleosome Structure

Nucleosomes are dynamic yet stable structures. The overall stability of a nucleosome depends on its constitution of the DNA sequence and histone composition. Although the early study by cross-linking and micrococcal digestion suggested the relative location of each histone protein (Karpov et al., 1982), the real breakthrough allowing one to see the detailed interactions is the crystalligraph data of a recombinant histone assembled onto a palindromic sequence at 2.8Å resolution (Luger et al., 1997). Each of the core histones contain the histone fold domain, which is composed of three α-helices connected by two loops. Heterodimers (H2A/H2B, H3/H4) interact with each other forming a handshake structure. The central tetramer forms through an H3-H3' four-helix bundle and the H2A/H2B dimers interact with the tetramer via H2B-H4 associations. Histone tails are exposed outside of the DNA and appear as disordered structure, which may function in internucleosome

interactions. Furthermore, a single arginine side chain was observed to insert into the minor groove at every turn of the DNA double helix.

This high resolution structure of nucleosome core particle provides important detail of the interactions between proteins and DNA. However, the absolute locations of histone-DNA interactions and their relative strengths are hard to obtain from the crystal structure. Complementary to crystal structure, Wang lab mechanically stretched (Brower-Toland et al., 2002) and unzipped (Shundrovsky et al., 2006; Hall et al., 2009) single DNA molecules containing a positioned nucleosome by utilizing an optical trap. Stretching data showed three regions of strong interactions within nucleosomes, with one around the dyad and the other two at ~40 bp away from the dyad. Unzipping data, together with the improved cross-correlation method, not only confirmed three regions of strong interactions, but also revealed a ~5 bp periodicity in each region of interactions, which, according to crystal structure, can be explained by the interactions between DNA minor groove and histone octamer surface from dsDNA every helical pitch. Moreover, the dwell times of unzipping fork at different sequences under constant force clamp indicated the relative strength of each interaction. As expected from the breathing model (Li and Widom, 2004), the unzipping fork did not dwell upon encountering entry and exit DNA. The strongest interactions have been found around dyad region. Interestingly, the third region of interactions was normally missing when unzipping proceeded from either direction, indicating that once the dyad region of interactions are disrupted, nucleosomes become unstable and likely to dissociate from the DNA. Furthermore, unzipping experiment also detected asymmetric interaction strengths from two opposite DNA ends, suggesting that

histone-DNA interactions are dependent on DNA underline sequence. In this study, the strong synthetic 601 nucleosome positioning sequence provided the homogeneous nucleosome population. However, whether nucleosomes assembled on different natural nucleosome positioning sequences share the same properties and the characterization of the protein-protein interactions remain to be answered.

RNAP Transcription through Nucleosomes

It is not hard to imagine that the compact nature of the nucleosomes inevitably impedes RNAP getting access to the genomic information buried in the nucleosome structure during transcription process. Indeed, in vitro studies have shown that transcription on chromatin template is slower than on naked DNA for all the RNAP model systems examined (Williamson and Felsenfeld, 1978; Izban and Luse, 1991; Studitsky et al., 1995; Studitsky et al., 1997; Kireeva et al., 2002; Walter et al., 2003; Xie and Reeve, 2004; Kireeva et al., 2005; Bondarenko et al., 2006; Ujvari et al., 2008). Interestingly, replacement of histones by tetramers significantly reduced the transcription barrier for T7 RNAP (Chirinos et al., 1999), but still formed a strong barrier for RNA polymerase II (Chang and Luse, 1997). Nucleosomal barriers can be alleviated by increasing salt concentrations (Williamson and Felsenfeld, 1978; Izban and Luse, 1991; Kireeva et al., 2002; Kireeva et al., 2005). Histone tails also play an important role in transcription. By removal of different combinations of histone tails and histone tail acetylations, the transcription rates for both T7 RNAP (Protacio et al., 2000) and yeast and human Pol II (Ujvari et al., 2008) are found to be increased. Unexpectedly, one to one

incorporation of linker histone H5 did not affect elongation efficiency for T7 RNAP transcription (Sanchez et al., 2003).

More in-depth studies focused not only on the transcription rate, but also on the mechanisms of transcription process and the fate of nucleosomes. For instance, yeast RNA polymerase III (Pol III), which primarily transcribes tRNA, was found to have a slower transcription rate on mononucleosomal template, but transcription was not prevented. Pol III proceeded with a pronounced pausing pattern ~ 10 – 11 bp periodicity. An enzyme digestion assay indicated that transcription induced a histone transfer over a distance of ~ 80 bp from one end of the transcription template to the other end (Studitsky et al., 1997). Bacteriaphage Sp6 RNAP, which has a smaller size, was also found to transfer histones but with less efficiency (Studitsky et al., 1995). Histone transfer was explained by a "spooling" model (Figure 1.6a), in which the RNAP first disrupts the ~ 25 bp of entries histone-DNA interactions without much hindrance; the exposal of the histone surface makes it possible for DNA behind the RNAP to bind, forming a DNA loop; this loop propagates along the histone surface as the RNAP transcribes, and it can be broken and reformed several times during the process; eventually, the RNAP trespasses the nucleosome, and the histone is transferred. Moreover, the observed 10-11 bp pausing periodicity was explained by rotational restriction of the RNAP due to the confined loop size. And the greater efficiency of histone transfer by Pol III was probably due to the slower transcription rate in comparison with Sp6 RNAP.

Kashlev's lab recently has developed a method to generate stalled Pol II

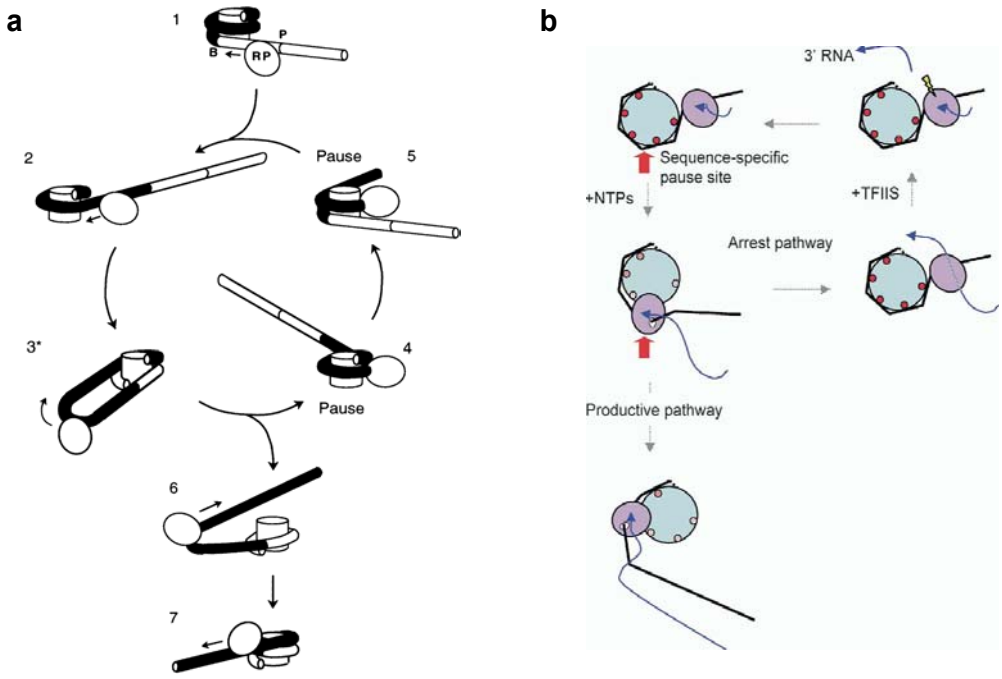

Figure 1.6. Proposed Models for Transcription through a Nucleosome (adapted from Bednar et al., 1999, and Kireeva et al., 2005)

(a) “Spooling” mechanism for Pol III transcription. 1. Pol III transcribes towards a nucleosome, 2. disrupts the first 25 bp histone-DNA interactions relatively easily, 3. DNA behind the Pol III forms a loop, 4. this loop can be broken and reformed several times, 5. leading to a paused complex, 6. if the downstream DNA-histone interactions are disrupted, 7. DNA-histone interactions can be restored by upstream DNA, completing transfer of the histone.

(b) Mechanism for Pol II transcription. Pol II unwinds the DNA from the surface of the histone octamer until it encounters an intrinsic pause site, which is likely to promote Pol II backtracking. TFIIS assists Pol II to be relieved from the backtracked state.

elongation complex without involving multiple initiation factors. By ligation of stalled elongation complex with a 5s rRNA sequence positioned nucleosome, they were able to study the RNAP behavior when it encounters a nucleosome (Kireeva et al., 2002; Kireeva et al., 2005). They showed that at or below physiological ionic strength (40 mM – 150 mM), the majority of the Pol II transcriptions were blocked by nucleosomal barriers. Increased ionic strength facilitated transcription potentially by destabilizing the nucleosome. At 300 mM salt, a novel complex was discovered after Pol II passage. By addition of H2A/H2B dimer, this novel complex restored the nucleosome. Furthermore, enzyme accessibility assay indicated that the novel complex was not transferred. Therefore, Pol II transcription induced H2A/H2B dimer loss, leaving a hexasome behind at the same location (Kireeva et al., 2002). Further study by the same group demonstrated that, in contrast to Pol III and Sp6 RNAP, nucleosome-induced pausing and arrest were mostly determined by the underlining DNA intrinsic pause sites. The restriction of Pol II rotation in the intranucleosomal DNA loop was not a prerequisite for those pauses. Moreover, TFIIS-induced Pol II active site digestion suggested that the presence of nucleosomes generated more long RNA products, consistent with Pol II backtracking upon nucleosomal barrier. Taken together, their data suggested that Pol II unwinds the DNA from the surface of the histone octamer until it encounters an intrinsic pause site, which is likely to promote Pol II backtracking. Factors that prevent Pol II backtracking or rescue Pol II from the backtracked state can facilitate transcription (Figure 1.6b) (Kireeva et al., 2005).

The properties of *E.coli* RNAP transcription through a nucleosome was also

studied although it does not encounter nucleosomes in prokaryotic cells. Interestingly, *E.coli* RNAP was reported to use similar mechanisms to go through nucleosomes. A nucleosome formed a significant barrier for *E.coli* RNAP transcription, and the presence of a nucleosome enhanced intrinsic pausing sites. *E.coli* RNAP transcription also induced H2A/H2B dimer loss, leaving a hexasome behind at the original location (Walter et al., 2003).

The above-mentioned studies used a natural gene sequence 5s rRNA to position a single nucleosome. Unfortunately, this sequence generates heterogeneity of two major nucleosome populations with 2 minor ones, which raises the difficulty of correlating transcription pauses respect to DNA sequences. In 1998, Widom and his co-workers carried out a SELEX experiment, and selected several DNA sequences (for instance, 601, 603, 605, etc.) which have high affinity for histones from a large pool of synthetic random DNA molecules. From then on, experiments which require a uniquely positioned nucleosome often use synthetic DNA to avoid ambiguity of nucleosome positioning. Pol II transcription through a mononucleosome positioned on 601, 603 and 605 was reported to have two major clusters of pauses, corresponding to + 15 and + 45 bp into the nucleosome (Bondarenko et al., 2006; Ujvari et al., 2008). Note that the front edge of Pol II is about 20 bp downstream of the pausing site, which indicates that the stalled positions of Pol II were actually at about 40 bp and 10 bp before the dyad. It was also found that transcription through the same nucleosome, but proceeding from opposite orientations encountered barriers with different strength. Since these synthetic DNA sequences are not palindromic, the polar barrier suggests that the barrier properties are also dictated by the strength of the histone-DNA

interactions (Bondarenko et al., 2006).

Despite the progress made previously, more transcription factors remain to be identified; more histone modifications remain to be discovered; transcription experiments are expected to be carried out in in vivo system with higher order chromatin structures which can more faithfully recapitulate physiological conditions. Nevertheless, understanding single RNAP transcription through a mononucleosome is the first step leading to the comprehension of regulatory role of the chromatin. In the next chapter, I will discuss single molecule study on the mechanism of RNAP transcription through a nucleosome and how RNAP itself can play an important role in trespassing nucleosomes.

REFERENCES

Abbondanzieri, E.A., Greenleaf, W.J., Shaevitz, J.W., Landick, R., and Block, S.M. (2005). Direct observation of base-pair stepping by RNA polymerase. Nature *438*, 460-465.

Alilat, M., Sivolob, A., Revet, B., and Prunell, A. (1999). Nucleosome dynamics. Protein and DNA contributions in the chiral transition of the tetrasome, the histone (H3-H4)2 tetramer-DNA particle. J Mol Biol *291*, 815-841.

Anderson, J.D., Lowary, P.T., and Widom, J. (2001). Effects of histone acetylation on the equilibrium accessibility of nucleosomal DNA target sites. J Mol Biol *307*, 977-985.

Anderson, J.D., and Widom, J. (2001). Poly(dA-dT) promoter elements increase the equilibrium accessibility of nucleosomal DNA target sites. Mol Cell Biol *21*, 3830-3839.

Bai, L., Fulbright, R.M., and Wang, M.D. (2007). Mechanochemical kinetics of transcription elongation. Phys Rev Lett *98*, 068103.

Belotserkovskaya, R., Oh, S., Bondarenko, V.A., Orphanides, G., Studitsky, V.M., and Reinberg, D. (2003). FACT facilitates transcription-dependent nucleosome alteration. Science *301*, 1090-1093.

Bondarenko, V.A., Steele, L.M., Ujvari, A., Gaykalova, D.A., Kulaeva, O.I., Polikanov, Y.S., Luse, D.S., and Studitsky, V.M. (2006). Nucleosomes can form a polar barrier to transcript elongation by RNA polymerase II. Mol Cell *24*, 469-479.

Brower-Toland, B.D., Smith, C.L., Yeh, R.C., Lis, J.T., Peterson, C.L., and Wang, M.D. (2002). Mechanical disruption of individual nucleosomes reveals a reversible multistage release of DNA. Proc Natl Acad Sci U S A *99*, 1960-1965.

Brown, C.E., Lechner, T., Howe, L., and Workman, J.L. (2000). The many HATs of transcription coactivators. Trends Biochem Sci *25*, 15-19.

Bruno, M., Flaus, A., Stockdale, C., Rencurel, C., Ferreira, H., and Owen-Hughes, T. (2003). Histone H2A/H2B dimer exchange by ATP-dependent chromatin remodeling activities. Mol Cell *12*, 1599-1606.

Chang, C.H., and Luse, D.S. (1997). The H3/H4 tetramer blocks transcript elongation by RNA polymerase II in vitro. J Biol Chem *272*, 23427-23434.

Chirinos, M., Hernandez, F., and Palacian, E. (1999). Transcription of DNA templates associated with histone (H3 x H4)(2) tetramers. Arch Biochem Biophys *370*, 222-230.

Galburt, E.A., Grill, S.W., Wiedmann, A., Lubkowska, L., Choy, J., Nogales, E., Kashlev, M., and Bustamante, C. (2007). Backtracking determines the force sensitivity of RNAP II in a factor-dependent manner. Nature *446*, 820-823.

Greive, S.J., and von Hippel, P.H. (2005). Thinking quantitatively about transcriptional regulation. Nat Rev Mol Cell Biol *6*, 221-232.

Hall, M.A., Shundrovsky, A., Bai, L., Fulbright, R.M., Lis, J.T., and Wang, M.D. (2009). High-resolution dynamic mapping of histone-DNA interactions in a nucleosome. Nat Struct Mol Biol *16*, 124-129.

Herbert, K.M., La Porta, A., Wong, B.J., Mooney, R.A., Neuman, K.C., Landick, R., and Block, S.M. (2006). Sequence-resolved detection of pausing by single RNA polymerase molecules. Cell *125*, 1083-1094.

Izban, M.G., and Luse, D.S. (1991). Transcription on nucleosomal templates by RNA polymerase II in vitro: inhibition of elongation with enhancement of sequence-specific pausing. Genes Dev *5*, 683-696.

Kapanidis, A.N., Margeat, E., Ho, S.O., Kortkhonjia, E., Weiss, S., and Ebright, R.H. (2006). Initial transcription by RNA polymerase proceeds through a DNA-scrunching mechanism. Science *314*, 1144-1147.

Karpov, V.L., Bavykin, S.G., Preobrazhenskaya, O.V., Belyavsky, A.V., and Mirzabekov, A.D. (1982). Alignment of nucleosomes along DNA and organization of spacer DNA in Drosophila chromatin. Nucleic Acids Res *10*, 4321-4337.

Kashlev, M., and Komissarova, N. (2002). Transcription termination: primary intermediates and secondary adducts. J Biol Chem *277*, 14501-14508.

Kassabov, S.R., Zhang, B., Persinger, J., and Bartholomew, B. (2003). SWI/SNF unwraps, slides, and rewraps the nucleosome. Mol Cell *11*, 391-403.

Kimura, H., and Cook, P.R. (2001). Kinetics of core histones in living human cells: little exchange of H3 and H4 and some rapid exchange of H2B. J Cell Biol *153*, 1341-1353.

Kireeva, M.L., Hancock, B., Cremona, G.H., Walter, W., Studitsky, V.M., and Kashlev, M. (2005). Nature of the nucleosomal barrier to RNA polymerase II. Mol Cell *18*, 97-108.

Kireeva, M.L., Walter, W., Tchernajenko, V., Bondarenko, V., Kashlev, M., and Studitsky, V.M. (2002). Nucleosome remodeling induced by RNA polymerase II: loss of the H2A/H2B dimer during transcription. Mol Cell *9*, 541-552.

Kobor, M.S., Venkatasubrahmanyam, S., Meneghini, M.D., Gin, J.W., Jennings, J.L., Link, A.J., Madhani, H.D., and Rine, J. (2004). A protein complex containing the conserved Swi2/Snf2-related ATPase Swr1p deposits histone variant H2A.Z into euchromatin. PLoS Biol *2*, E131.

Komissarova, N., and Kashlev, M. (1997). Transcriptional arrest: Escherichia coli RNA polymerase translocates backward, leaving the 3' end of the RNA intact and extruded. Proc Natl Acad Sci U S A *94*, 1755-1760.

Konev, A.Y., Tribus, M., Park, S.Y., Podhraski, V., Lim, C.Y., Emelyanov, A.V., Vershilova, E., Pirrotta, V., Kadonaga, J.T., Lusser, A.*, et al.* (2007). CHD1

motor protein is required for deposition of histone variant H3.3 into chromatin in vivo. Science *317*, 1087-1090.

Koyama, H., Nagao, T.A., Inai, T., Miyahara, K., Hayasida, Y., Shirahige, K., and Tsuchiya, E. (2004). RSC Nucleosome-remodeling complex plays prominent roles in transcriptional regulation throughout budding yeast gametogenesis. Biosci Biotechnol Biochem *68*, 909-919.

Larson, M.H., Greenleaf, W.J., Landick, R., and Block, S.M. (2008). Applied force reveals mechanistic and energetic details of transcription termination. Cell *132*, 971-982.

Lesnik, E.A., Sampath, R., Levene, H.B., Henderson, T.J., McNeil, J.A., and Ecker, D.J. (2001). Prediction of rho-independent transcriptional terminators in Escherichia coli. Nucleic Acids Res *29*, 3583-3594.

Levchenko, V., Jackson, B., and Jackson, V. (2005). Histone release during transcription: displacement of the two H2A-H2B dimers in the nucleosome is dependent on different levels of transcription-induced positive stress. Biochemistry *44*, 5357-5372.

Li, G., and Widom, J. (2004). Nucleosomes facilitate their own invasion. Nat Struct Mol Biol *11*, 763-769.

Luger, K., Mader, A.W., Richmond, R.K., Sargent, D.F., and Richmond, T.J. (1997). Crystal structure of the nucleosome core particle at 2.8 A resolution. Nature *389*, 251-260.

Mejia, Y.X., Mao, H., Forde, N.R., and Bustamante, C. (2008). Thermal probing of E. coli RNA polymerase off-pathway mechanisms. J Mol Biol *382*, 628-637.

Mizuguchi, G., Shen, X., Landry, J., Wu, W.H., Sen, S., and Wu, C. (2004). ATP-driven exchange of histone H2AZ variant catalyzed by SWR1 chromatin remodeling complex. Science *303*, 343-348.

Moffitt, J.R., Chemla, Y.R., Izhaky, D., and Bustamante, C. (2006). Differential detection of dual traps improves the spatial resolution of optical tweezers. Proc Natl Acad Sci U S A *103*, 9006-9011.

Mozziconacci, J., and Victor, J.M. (2003). Nucleosome gaping supports a functional structure for the 30nm chromatin fiber. J Struct Biol *143*, 72-76.

Nudler, E., and Gottesman, M.E. (2002). Transcription termination and anti-termination in E. coli. Genes Cells *7*, 755-768.

Pennings, S., Muyldermans, S., Meersseman, G., and Wyns, L. (1989). Formation, stability and core histone positioning of nucleosomes reassembled on bent and other nucleosome-derived DNA. J Mol Biol *207*, 183-192.

Protacio, R.U., Li, G., Lowary, P.T., and Widom, J. (2000). Effects of histone tail domains on the rate of transcriptional elongation through a nucleosome. Mol Cell Biol *20*, 8866-8878.

Rasnik, I., McKinney, S.A., and Ha, T. (2006). Nonblinking and long-lasting single-molecule fluorescence imaging. Nat Methods *3*, 891-893.

Revyakin, A., Liu, C., Ebright, R.H., and Strick, T.R. (2006). Abortive initiation and productive initiation by RNA polymerase involve DNA scrunching. Science *314*, 1139-1143.

Richardson, L.V., and Richardson, J.P. (1996). Rho-dependent termination of transcription is governed primarily by the upstream Rho utilization (rut) sequences of a terminator. J Biol Chem *271*, 21597-21603.

Sanchez, M.A., Velasco, L., and Palacian, E. (2003). Structure-function relationships in nucleosomal arrays containing linker histone H5. Biochim Biophys Acta *1628*, 177-185.

Schafer, D.A., Gelles, J., Sheetz, M.P., and Landick, R. (1991). Transcription by single molecules of RNA polymerase observed by light microscopy. Nature *352*, 444-448.

Shaevitz, J.W., Abbondanzieri, E.A., Landick, R., and Block, S.M. (2003). Backtracking by single RNA polymerase molecules observed at near-base-pair resolution. Nature *426*, 684-687.

Shundrovsky, A., Santangelo, T.J., Roberts, J.W., and Wang, M.D. (2004). A single-molecule technique to study sequence-dependent transcription pausing. Biophys J *87*, 3945-3953.

Shundrovsky, A., Smith, C.L., Lis, J.T., Peterson, C.L., and Wang, M.D. (2006). Probing SWI/SNF remodeling of the nucleosome by unzipping single DNA molecules. Nat Struct Mol Biol *13*, 549-554.

Smith, C.L., and Peterson, C.L. (2005). ATP-dependent chromatin remodeling. Curr Top Dev Biol *65*, 115-148.

Studitsky, V.M., Clark, D.J., and Felsenfeld, G. (1995). Overcoming a nucleosomal barrier to transcription. Cell *83*, 19-27.

Studitsky, V.M., Kassavetis, G.A., Geiduschek, E.P., and Felsenfeld, G. (1997). Mechanism of transcription through the nucleosome by eukaryotic RNA polymerase. Science *278*, 1960-1963.

Thiriet, C., and Hayes, J.J. (2005). Replication-independent core histone dynamics at transcriptionally active loci in vivo. Genes Dev *19*, 677-682.

Tomschik, M., van Holde, K., and Zlatanova, J. (2009). Nucleosome dynamics as studied by single-pair fluorescence resonance energy transfer: a reevaluation. J Fluoresc *19*, 53-62.

Toulme, F., Mosrin-Huaman, C., Sparkowski, J., Das, A., Leng, M., and Rahmouni, A.R. (2000). GreA and GreB proteins revive backtracked RNA polymerase in vivo by promoting transcript trimming. EMBO J *19*, 6853-6859.

Ujvari, A., Hsieh, F.K., Luse, S.W., Studitsky, V.M., and Luse, D.S. (2008). Histone N-terminal tails interfere with nucleosome traversal by RNA polymerase II. J Biol Chem *283*, 32236-32243.

Walter, W., Kireeva, M.L., Studitsky, V.M., and Kashlev, M. (2003). Bacterial polymerase and yeast polymerase II use similar mechanisms for transcription through nucleosomes. J Biol Chem *278*, 36148-36156.

Wang, M.D., Schnitzer, M.J., Yin, H., Landick, R., Gelles, J., and Block, S.M. (1998). Force and velocity measured for single molecules of RNA polymerase. Science *282*, 902-907.

Whitehouse, I., Stockdale, C., Flaus, A., Szczelkun, M.D., and Owen-Hughes, T. (2003). Evidence for DNA translocation by the ISWI chromatin-remodeling enzyme. Mol Cell Biol *23*, 1935-1945.

Williamson, P., and Felsenfeld, G. (1978). Transcription of histone-covered T7 DNA by Escherichia coli RNA polymerase. Biochemistry *17*, 5695-5705.

Woudstra, E.C., Gilbert, C., Fellows, J., Jansen, L., Brouwer, J., Erdjument-Bromage, H., Tempst, P., and Svejstrup, J.Q. (2002). A Rad26-Def1 complex

coordinates repair and RNA pol II proteolysis in response to DNA damage. Nature *415*, 929-933.

Xie, Y., and Reeve, J.N. (2004). Transcription by an archaeal RNA polymerase is slowed but not blocked by an archaeal nucleosome. J Bacteriol *186*, 3492-3498.

Yang, J.G., Madrid, T.S., Sevastopoulos, E., and Narlikar, G.J. (2006). The chromatin-remodeling enzyme ACF is an ATP-dependent DNA length sensor that regulates nucleosome spacing. Nat Struct Mol Biol *13*, 1078-1083.

Yin, H., Artsimovitch, I., Landick, R., and Gelles, J. (1999). Nonequilibrium mechanism of transcription termination from observations of single RNA polymerase molecules. Proc Natl Acad Sci U S A *96*, 13124-13129.

Yin, H., Landick, R., and Gelles, J. (1994). Tethered particle motion method for studying transcript elongation by a single RNA polymerase molecule. Biophys J *67*, 2468-2478.

Zhang, G., Campbell, E.A., Minakhin, L., Richter, C., Severinov, K., and Darst, S.A. (1999). Crystal structure of Thermus aquaticus core RNA polymerase at 3.3 A resolution. Cell *98*, 811-824.

Zhang, Y., Smith, C.L., Saha, A., Grill, S.W., Mihardja, S., Smith, S.B., Cairns, B.R., Peterson, C.L., and Bustamante, C. (2006). DNA translocation and loop

formation mechanism of chromatin remodeling by SWI/SNF and RSC. Mol Cell *24*, 559-568.

CHAPTER TWO:
SINGLE MOLECULE STUDY ON RNA POLYMERASE TRANSCRIPTION THROUGH MONONUCLEOSOME

INTRODUCTION

Nucleosomes are known to play an important role in the regulation of gene expression. During transcription, eukaryotic RNA polymerase (RNAP) must access DNA associated with nucleosomes, the fundamental packing units of chromatin. In vitro studies have shown that nucleosomes impose substantial barriers to transcription elongation by a single RNAP (Izban and Luse, 1991; Studitsky et al., 1995; Studitsky et al., 1997; Walter and Studitsky, 2001; Kireeva et al., 2002; Walter et al., 2003; Kireeva et al., 2005; Bondarenko et al., 2006; Ujvari et al., 2008). Even a mononucleosome can effectively block the passage of yeast RNA polymerase II (Pol II) under physiological salt concentrations (Kireeva et al., 2002; Kireeva et al., 2005; Ujvari et al., 2008). The presence of a nucleosome induces Pol II to pause/arrest due to backtracking, during which Pol II disengages its active site from the 3' end of RNA and slides backwards non-catalytically along the DNA, resulting in an extrusion of 3' RNA through its secondary channel (Kireeva et al., 2005).

Whereas in vitro studies suggest the difficulty of Pol II transcription through chromatin, in vivo data have shown that Pol II elongates at 20-80 bp/s without much discontinuity even in the presence of nucleosomes (O'Brien and Lis, 1993; Tennyson et al., 1995; Darzacq et al., 2007). If so, how does Pol II overcome the nucleosome barrier during elongation? To date, several mechanisms that facilitate Pol II transcription through nucleosomes have been recognized. One mechanism involves enzymes which directly regulate Pol II's elongation rate and efficiency. For example, TFIIS is capable of binding to the secondary channel of Pol II, facilitating the cleavage of RNA by Pol II to realign

the 3' end with the active site, and thus allowing arrested ternary complexes to resume transcription (Awrey et al., 1998; Weilbaecher et al., 2003; Kireeva et al., 2005; Galburt et al., 2007). Other mechanisms involve various types of nucleosome modifications to make the DNA more accessible in a nucleosome. For example, histone acetyltransferases are found to acetylate conserved lysine residues in histones so as to reduce the affinity between the histones and DNA (Brown et al., 2000; Anderson et al., 2001; Roth et al., 2001). In addition, nucleosome-remodeling enzymes and histone chaperones have been shown to reposition nucleosomes and to evict histones out of the path of transcription (Belotserkovskaya et al., 2003; Schwabish and Struhl, 2007).

Nudler and colleagues have hypothesized that cooperation by multiple RNAPs may also contribute to efficient RNAP progression through a nucleosomal barrier (Epshtein et al., 2003). There is no direct experimental evidence for this hypothesis; however, several observations suggest that it may be plausible. First, a number of in vivo and in vitro studies show that for highly expressed genes, multiple initiation is a common strategy to increase transcription efficiency in cells (Lee et al., 2004; Varv et al., 2007). Second, biochemical studies of *E. coli* RNAP show that when multiple initiation takes place from the same promoter, the leading RNAP is able to more efficiently forward translocate through a bound protein such as *Eco*RQ111 or *lac* repressor, with a concomitant reduction in the RNAP arrest probability (Epshtein et al., 2003; Toulme et al., 2005). Third, single molecule studies show that both *E. coli* RNAP and Pol II are powerful molecular motors, capable of exerting forces and generating displacements (Wang et al., 1998; Galburt et al., 2007). Thus an assisting force may be exerted by a trailing

RNAP on a leading RNAP as the leading RNAP encounters a nucleosome barrier. Indeed an assisting external force has been shown to reduce RNAP backtracking while facilitating its forward translocation (Shundrovsky et al., 2004; Galburt et al., 2007).

Here we have tested this hypothesis using *E. coli* RNAP as a model system. *E. coli* RNAP is structurally simpler than Pol II and requires only the holoenzyme for initiation. Pol II and *E.coli* RNAP are both responsible for transcribing mRNA, and their core is evolutionarily conserved in sequence, structure and function from bacteria to human (Ebright, 2000; Korzheva and Mustaev, 2001). Although *E. coli* does not contain chromatin, its RNAP must deal with histone-like proteins during transcription (Lathe et al., 1980; Balandina et al., 2002). Remarkably, *E. coli* RNAP resembles yeast Pol II in all tested properties of transcription through a nucleosome in vitro (Walter et al., 2003). For instance, *E. coli* RNAP is also known to backtrack (Komissarova and Kashlev, 1997; Toulme et al., 2000; Shaevitz et al., 2003), encounter a major barrier at a nucleosome, and pause at essentially identical sites to those of Pol II at a nucleosome (Walter et al., 2003). Thus *E. coli* RNAP has been viewed as a suitable model system to study transcription through nucleosomes by Pol II.

In this work, we ascertained how two RNAPs may work together to transcribe through a nucleosome. This was achieved by monitoring the physical location of an RNAP along a nucleosomal DNA to within a few base pairs using a single molecule DNA unzipping technique, and assaying the corresponding RNA transcript length using a bulk transcription technique. We first compared

the RNAP pausing pattern when it encountered a nucleosome with histone-DNA interaction maps that we previously determined (Hall et al., 2009). The strong correlation between them led us to conclude that RNAP pausing at a nucleosome is dictated primarily by the histone-DNA interactions. Second, we determined the backtracking distance of RNAP when it encountered a nucleosome and found it to be on average ~ 10-15 bp. Third, we simultaneously monitored the locations of two RNAPs, both moving towards a nucleosome. We found that the trailing RNAP was capable of exerting an assisting force on the leading RNAP, reducing its backtracking and enhancing its elongation rate through a nucleosome 5-fold. The trailing RNAP also had a 2-fold rate enhancement compared with that from a single RNAP working alone.

RESULTS

Determine RNAP Footprint by Mechanical Unzipping

It has been demonstrated that the mechanical unzipping of double-strand (ds) DNA is a powerful tool to study DNA-protein interactions. By using the unzipping method, we have previously reported a high resolution nucleosome-DNA interaction map (Hall et al., 2009). Here, we use the same method to investigate the accurate RNAP footprint on nucleosome template. We constructed an unzipping template which can be unzipped from both ends. This template contains a T7A1 promoter which recruits RNAP (Figure 2.2b). Pause transcription complex (PTC) was formed by incubating RNAP with subset of four NTPs at 37ºC for 20 min to walk RNAP to +20 nt. To unzip

DNA through a PTC, an optical trap was used to sequentially convert dsDNA into ssDNA by mechanical separation of base pairs (Figure 2.1; Experimental Procedures). An RNAP-DNA interaction was detected whenever the unzipping force significantly deviated from the corresponding naked DNA unzipping force, a sequence-dependent baseline around 15 pN.

When a single DNA molecule was unzipped starting from upstream of the RNAP (Figure 2.2a, upper panel), the unzipping force initially followed that of the corresponding naked DNA. However, as the unzipping fork approached the RNAP, the force dropped below the naked DNA baseline and this was immediately followed by a sharp force rise above the baseline. The unzipping force then continued to follow that of the corresponding naked DNA. We interpret the onset of the force drop as the unzipping fork encountering the transcription bubble formed by RNAP, and the location of the subsequent force rise as the end of the transcription bubble and the beginning of the dsDNA that was clamped downstream by the RNAP. The magnitude of the force drop and the rise varied from trace to trace as would be expected from a thermally activated, off-equilibrium process. Similarly, when the unzipping started from the downstream of the RNAP (Figure 2.2a, bottom panel), only a force rise was observed. We interpret this force rise as the onset of the RNAP interaction with the downstream dsDNA. Since the large tension built up during the force rise was relaxed over a long distance, the transcription bubble could not be detected.

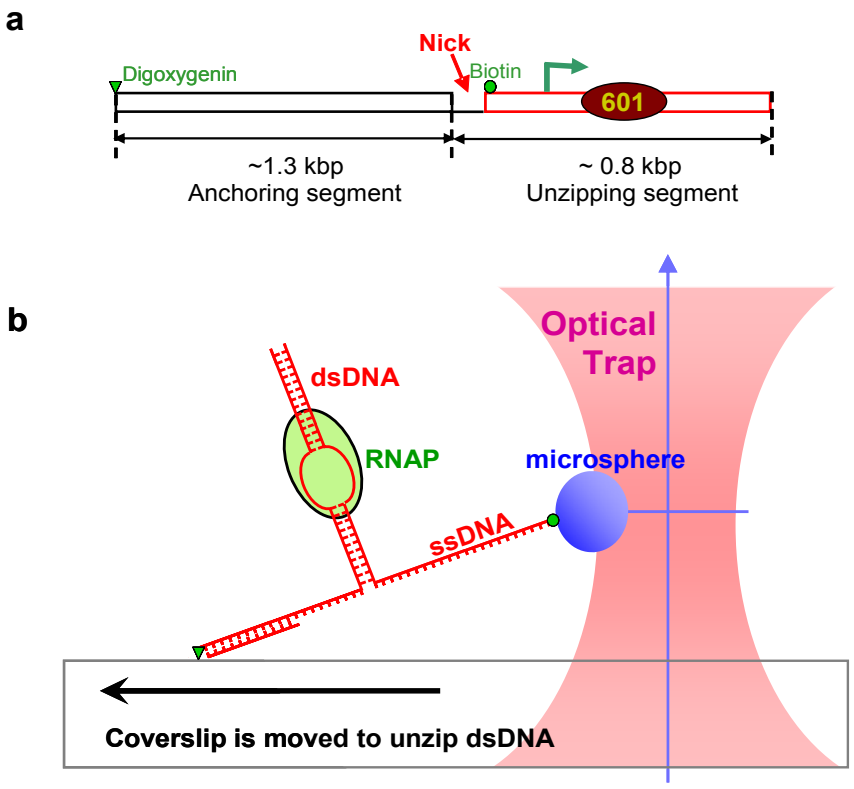

Figure 2.1. Experimental Setup

(a) Each DNA template for single molecule experiments consisted of an anchoring segment and an unzipping segment, which were ligated together leaving a nick at the ligation site. As illustrated by a single-promoter template here, the anchoring segment was dig-labeled at the distal end, while the unzipping segment was labeled with a biotin 5 bp away from the nick.

(b) The DNA template was attached at one end to the surface of a glass coverslip via a digoxigenin-antidigoxigenin linkage and at its nick to a microsphere via a biotin-streptavidin linkage. As the coverslip was moved away from the trapped microsphere, the dsDNA was sequentially converted into ssDNA upon base pair separation.

Figure 2.2. Unzipping Force Signature of a Paused Transcription Elongation Complex

(a) Unzipping DNA through a paused transcription complex from both the forward (top panel) and reverse (bottom panel) directions. The unzipping force of the corresponding naked DNA in both directions is shown for comparison (grey). Three characteristic locations are highlighted. In the forward unzipping direction, the onset of the force drop should correspond to the beginning of the transcription bubble, and the subsequent force rise should correspond to the end of the transcription bubble and the beginning of the dsDNA clamped by RNAP. In the reverse unzipping direction, the force rise corresponds to the onset of the RNAP interaction with the downstream dsDNA.

(b) A cartoon of the transcription elongation complex.

(c) An RNAP-DNA interaction map for the transcription elongation complex. Three histograms were obtained by pooling a number of measurements such as those shown in (A). They show the onset of the force drop (N = 32) and the force rise peak (N = 32) in the forward unzipping direction, and the force rise peak (N = 20) in the reverse unzipping direction. The mean position of each histogram is indicated by a dashed line. The transcription bubble size was measured to be ~ 18 bp, and the length of the downstream dsDNA region in the elongation complex ~18 bp.

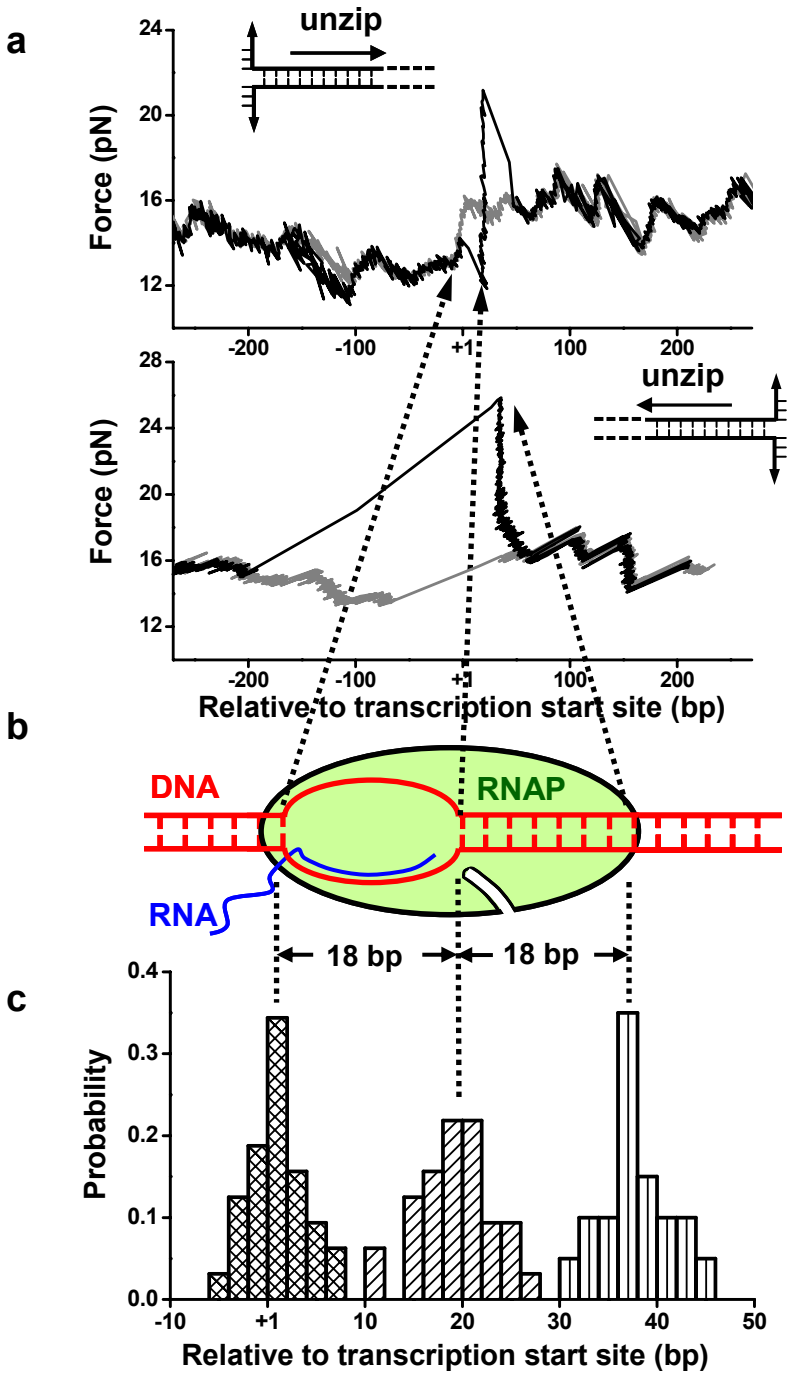
a
unzip
Force (pN)
24
20
16
12
-200
-100
+1
100
200
28
24
20
16
12
unzip
Relative to transcription start site (bp)
b
DNA
RNAP
RNA
18 bp
18 bp
c
Probability
0.4
0.3
0.2
0.1
0.0
-10
+1
10
20
30
40
50
Relative to transcription start site (bp)

An RNAP-DNA interaction map (Figure 2.2c) was generated by pooling data from a number of such measurements to obtain the location of the onset of the force drop and the peak location of the force rise from unzipping in the forward direction, and the peak location of the force rise from unzipping in the reverse location. This map suggests that in an elongation complex the transcription bubble is ~18 bp and RNAP clamps ~ 18 bp of the downstream dsDNA. The measured bubble size is on the large side of the previous biochemical studies (14 –18 bp) (Lee and Landick, 1992; Zaychikov et al., 1997; Pal et al., 2005). Spontaneous opening of the unzipping fork under thermal fluctuations might have caused advance sensing of the bubble. The measured length of the downstream dsDNA region in the elongation complex is consistent with previously measured values (16 – 21 bp).

For a PTC at +20 nt, the active site of the RNAP is expected to be at +20 bp from the transcription start site and the downstream dsDNA is expected to begin at around + (23 ± 1) bp (Zaychikov et al., 1995; Nudler et al., 1998; Korzheva et al., 2000). However, the location of the force rise, indicative of the beginning of the downstream dsDNA, was detected at + (19.4 ± 4.0) bp (mean ± sd) (Figure 2.2c, center histogram, and Figure 2.3a). This slight upstream shift from the expected location of the force rise was because a fraction of the PTCs was backtracked due to NTP starvation (Figure A.3). This backtracking also generated a broadening of the force rise location distribution. However, for a given single molecule measurement, the force rise was determined to an accuracy and precision of ~ 1.5 bp (Hall et al., 2009).

Locating RNAP by Unzipping DNA

In order to more accurately reflect an RNAP physical location along DNA when RNAP progresses through a nucleosome, we needed to minimize RNAP diffusive motion along the DNA in a stalled elongation complex. This was achieved by forming PTC at room temperature for 2 min, and then immediately quenched by EDTA. Shorter incubation time and lower temperature allowed a fraction of RNAP to form PTC, but mostly thermally confined to the designed location. Unzipping experiments from the upstream DNA were followed to determine the location of the force rise, which is an indication of the beginning of the downstream dsDNA. Indeed, the force rise was detected at +22 bp (Figure 2.3b), in excellent agreement with the expected location. To examine whether depletion of Mg^{2+} by EDTA quenching can preserve the RNAP translocation state, the above mentioned elongation complexes were further incubated at 37ºC for 30 min, which was supposed to encourage RNAP diffusion. Unzipping experiments revealed that both the mean location and the standard deviation of the RNAP locations were essentially unaltered (Figure 2.3c), indicating that depletion of Mg^{2+} by EDTA quenching inhibits RNAP diffusive translocation in a stalled elongation complex even under thermally favored conditions. Thus the unzipping force signature of an RNAP serves as a convenient and distinctive indicator of the RNAP location. The active site location was then taken to be 2 bp upstream from the measured force rise location for all subsequent experiments. It is worth noting that an RNAP physical location along DNA can not be readily located by conventional bulk transcription gel assays which measure the length of the RNA transcript, i.e., the 3' RNA location along the DNA.

Figure 2.3. Inhibition of RNAP Diffusive Translocation by Depletion of Mg^{2+}

Unzipping experiments from upstream of the DNA were performed to compare RNAP force rise locations in the PTC formed under three different conditions. The mean position of each distribution is indicated by an arrow.

(a) PTC formation for 20 min at 37ºC (Experimental Procedures) is known to encourage RNAP backtracking. Indeed, the mean position of the RNAP location distribution was found to be ~ +19 bp, outside the range of the expected range of location (+22-24 bp).

(b) PTC was allowed to form under room temperature (RT) and quenched after 2 min by EDTA. The mean position of the RNAP location distribution was found to be at ~ +22 bp, within the range of the expected range of location.

(c) The same experiment began as in Figure b, and was followed by a further incubation at 37ºC for 30 min. Unzipping experiments revealed that both the mean location and the standard deviation of the RNAP locations were essentially unaltered, indicating that depletion of Mg^{2+} by EDTA quenching indeed inhibits RNAP diffusive translocation in an elongation complex.

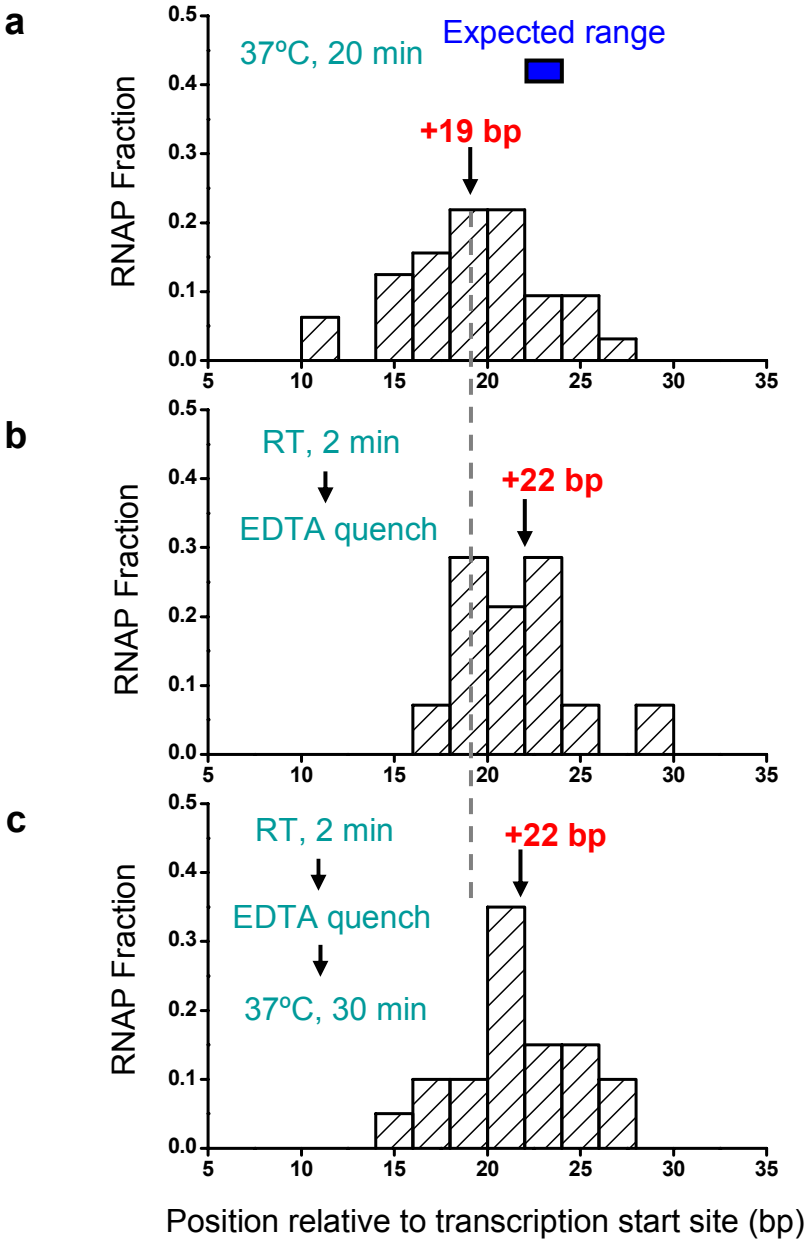
a
37ºC, 20 min
Expected range
+19 bp
RNAP Fraction
b
RT, 2 min
EDTA quench
+22 bp
RNAP Fraction
c
RT, 2 min
EDTA quench
37ºC, 30 min
+22 bp
RNAP Fraction
0.0
0.1
0.2
0.3
0.4
0.5
5
10
15
20
25
30
35
Position relative to transcription start site (bp)

Locating RNAP during Elongation on Nucleosomal DNA

We next demonstrated that the DNA unzipping assay could also be used to locate an RNAP during elongation on nucleosomal DNA. For these experiments, we constructed a DNA template containing a single T7A1 promoter followed by a 601 nucleosome positioning element (NPE) that is known to uniquely position a nucleosome (Lowary and Widom, 1998; Widom, 2001) (Figure 2.4a). Note that the 601 NPE was flanked by long stretches of DNA, in contrast to short DNA templates typically used in conventional biochemistry experiments. We then assembled a single nucleosome onto the 601 NPE using a salt dialysis method and subsequently formed a PTC at the +20 nt position (Experimental Procedures). When this DNA template containing a PTC and a nucleosome was unzipped, the characteristic force signatures for both the RNAP and the nucleosome were observed at their expected locations (Figure 2.2b).

Previously we have fully characterized the histone-DNA interactions within a nucleosome using the DNA unzipping method (Hall et al., 2009). The unzipping force signatures of the nucleosomes observed here were consistent with the previous results. The nucleosome was uniquely positioned within the 601 NPE. For a given nucleosome, there were three broad regions of strong interactions, with one around the dyad and the other two around ~ $\pm$40 bp from the dyad. Unzipping from one direction typically only revealed the first two regions encountered but not the last one, due to histone dissociation from the 601 NPE upon disruption of the dyad region of interactions.

Figure 2.4. Locating an RNAP during Elongation on Nucleosomal DNA

(a) The single-promoter transcription template construct containing both a single T7A1 promoter and a 601 nucleosome positioning element (NPE).

(b) An example unzipping trace of a template containing both a PTC stalled at +20 nt and a positioned nucleosome. Unzipping confirmed that the RNAP and the nucleosome were at their expected locations. Two regions of strong histone-DNA interactions in a nucleosome are indicated: Region 1 (off-dyad interactions) and Region 2 (dyad interactions). The brown bar indicates the 147-bp 601 NPE.

(c) Representative traces of unzipping through an elongation complex. After transcription was resumed for an indicated duration, it was quenched and histones were dissociated. Unzipping revealed the location of the remaining RNAP. Each trace is from a different DNA molecule. The unzipping force of the corresponding naked DNA is shown for comparison (grey).

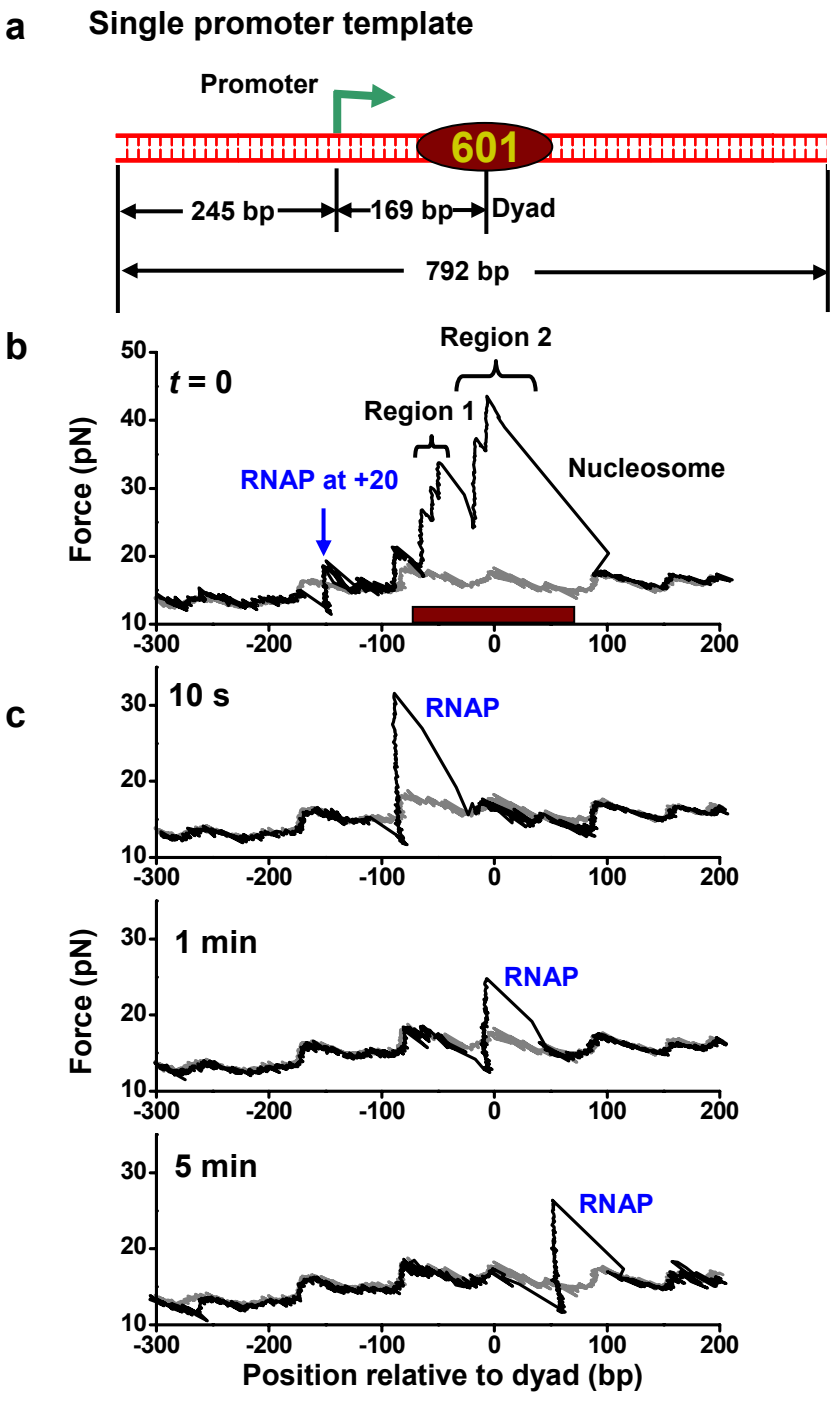
a
Single promoter template
Promoter
601
245 bp
169 bp
Dyad
792 bp
b
Region 2
t = 0
Region 1
RNAP at +20
Nucleosome
Force (pN)
c
10 s
RNAP
1 min
RNAP
5 min
RNAP
Position relative to dyad (bp)

In order to monitor the location of an RNAP elongating through a nucleosome, elongation was resumed by supplementing the reaction buffer with 1 mM of NTPs, together with competitor DNA containing a T7A1 promoter to prevent re-initiation (Experimental Procedures, Figure A.1). The reaction was then quenched by excess EDTA at specified time points. When the RNAP was not in the immediate vicinity of the nucleosome, the unzipping force signatures for both the RNAP and the nucleosome were readily discernable (as shown in Figure 2.4b). However when the RNAP had encountered a nucleosome, we observed a much more complex and variable force signature that did not readily distinguish between the RNAP and the nucleosome. To examine only the RNAP location, heparin was used to dissociate the histones from the DNA immediately *after* the chase reaction was quenched (Experimental Procedures). Control experiments were carried out to show that the heparin concentration used was sufficient to completely dissociate a positioned nucleosome (Figure A.2a and legend). In addition, neither the competitor DNA nor heparin dissociated RNAP or altered RNAP locations (Figure A.1 legend, A.2b). Figure 2.4c shows some representative traces from DNA molecules at three transcription times. As RNAP moved through a nucleosome, it encountered strong interactions preceding the dyad region (10 s trace) followed by strong interactions at the dyad region (1 min trace), and then moved out of the nucleosome (5 min trace).

Transcription Pausing is Induced by Strong Histone-DNA Interactions within a Nucleosome

Previous studies indicate that when RNA polymerase III (Pol III) encounters a nucleosome, a DNA loop is formed between the nucleosome and the DNA upstream of the RNAP (Studitsky et al., 1997). The loop restricts the rotation of the RNAP around the DNA helical axis as it translocates along the DNA and thus induces transcription pausing at a 10-11 bp periodicity, the helical pitch of the DNA. On the other hand, it has been shown that DNA loop formation is not a prerequisite for nucleosome-induced transcription pausing and arrest for Pol II (Kireeva et al., 2005). Instead, these studies suggest that Pol II pauses mostly at intrinsic pause sites while the presence of a nucleosome promotes the conversion of transient short pauses into long pauses and arrests. In addition, Pol II was not reported to pause with any periodicity. However, these conclusions were based on experiments that used a weak NPE which is known to generate nucleosome positioning heterogeneity and thus may have obscured important features of pausing.

Therefore we first carefully examined nucleosome-induced pause sites using a uniquely positioned nucleosome and bulk transcription assays on a DNA template prepared identically to that used for Figure 2.4a (Figure 2.5a, top). The PTCs were chased with 1 mM NTPs for specified time durations before the reaction was quenched by excess EDTA (Experimental Procedures). Subsequently the lengths of the RNA, indicative of the 3' end location of the RNA transcript on DNA, were determined using denaturing PAGE. As shown in Figure 2.5a (bottom), the presence of a nucleosome dramatically reduced

Figure 2.5. Transcription through a Nucleosome Shows a Distinctive 10 bp Periodicity Pausing Pattern

(a) RNAP transcribed through a nucleosome in the forward direction of the 601NPE as indicated by the template cartoon (identical to Figure 2.4a). PAGE analysis of transcription through naked DNA and nucleosomal DNA shows that as RNAP proceeded into the nucleosome, a distinctive periodicity of ~ 10 bp highlighted all nucleosome-induced pause sites within Regions 1 and 2. Transcription pause sites are marked as distances from the dyad.

(b) RNAP transcribed through a nucleosome from the reverse direction of 601NPE as indicated by the template cartoon. Although RNAP effectively transcribed a different sequence, all nucleosome-induced pauses were again highlighted by a distinctive ~ 10 bp periodicity within Regions 1 and 2. The pause site at the end of the 601NPE might be intrinsic pausing (compare transcription through naked DNA and nucleosomal DNA). Also note that at this pause site the leading edge of the RNAP was ~ 20 bp downstream of the 601 NPE.

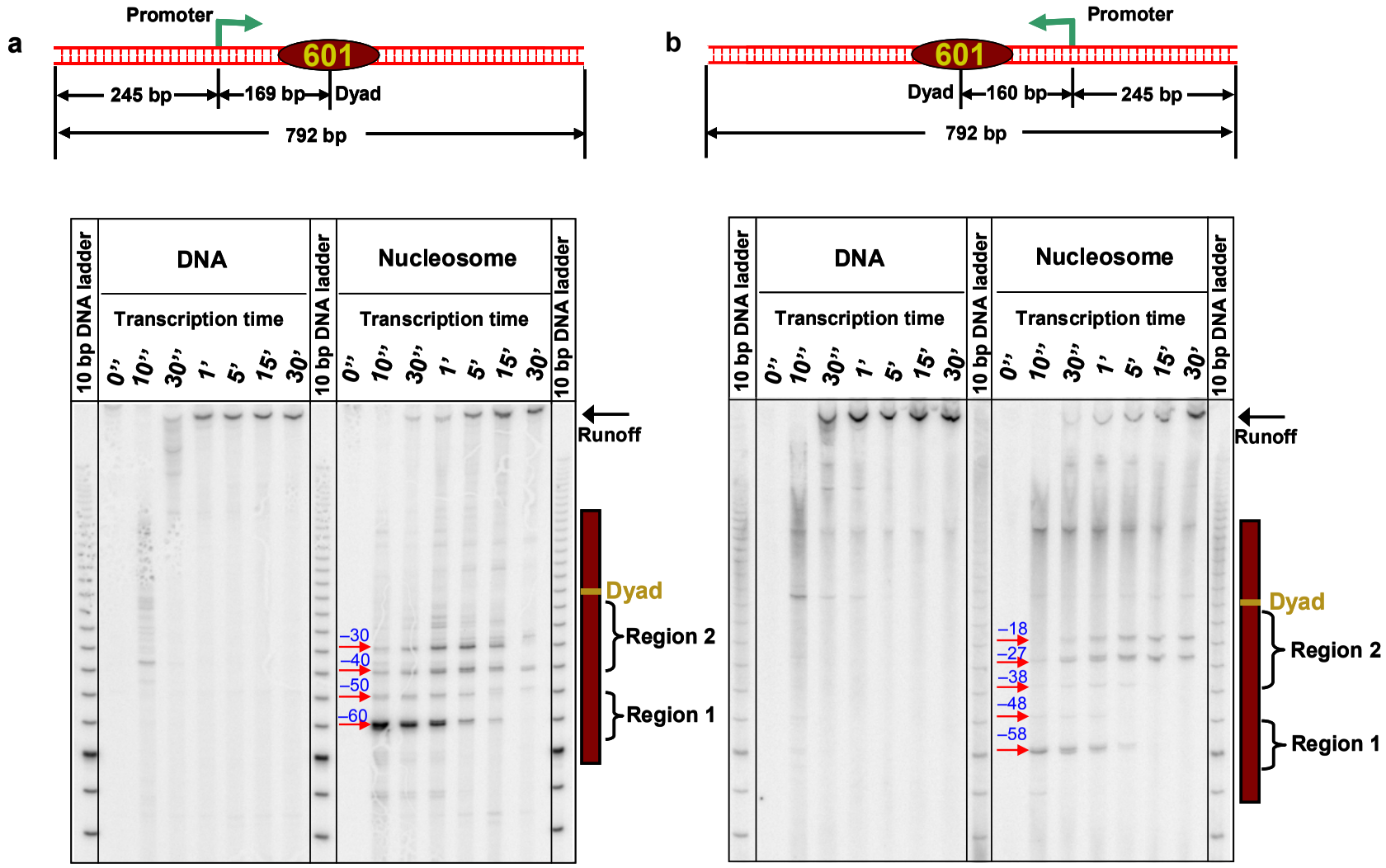
a
Promoter
601
245 bp
169 bp
Dyad
792 bp
b
Promoter
601
Dyad
160 bp
245 bp
792 bp
10 bp DNA ladder
DNA
Transcription time
0'' 10'' 30'' 1' 5' 15' 30'
10 bp DNA ladder
Nucleosome
Transcription time
0'' 10'' 30'' 1' 5' 15' 30'
10 bp DNA ladder
Runoff
Dyad
Region 2
Region 1
−30
−40
−50
−60
10 bp DNA ladder
DNA
Transcription time
0'' 10'' 30'' 1' 5' 15' 30'
10 bp DNA ladder
Nucleosome
Transcription time
0'' 10'' 30'' 1' 5' 15' 30'
10 bp DNA ladder
Runoff
Dyad
Region 2
Region 1
−18
−27
−38
−48
−58

the transcription rate, consistent with previous observations (Izban and Luse, 1991; Walter and Studitsky, 2001; Kireeva et al., 2002; Walter et al., 2003; Kireeva et al., 2005; Bondarenko et al., 2006; Ujvari et al., 2008). While essentially all RNAPs reached the runoff end of a naked DNA template within 1 min, only ~ 50% of RNAPs were able to reach the runoff end in the presence of a nucleosome, even after 30 min. In addition, as RNAP proceeded into the nucleosome, a distinct periodicity of ~ 10 bp highlighted the nucleosome-induced pause sites.

The pause sites should correspond to resistance from histone-DNA interactions that are encountered by the RNAP leading edge located at ~ 20 bp downstream of the active site (Samkurashvili and Luse, 1996). As shown in Figure 2.5a, when RNAP encountered the nucleosome, it paused strongly at –60 bp from the dyad corresponding to the off-dyad region of strong interactions (Region 1). Upon escaping from this pause, it paused again at –50 bp (weak), –40 bp (strong) and –30 bp (strongest) from the dyad corresponding to the dyad region of strong interactions (Region 2). As the front of the RNAP passed the dyad region, pausing immediately disappeared, indicating the absence of major obstacles.

To determine if the RNAP pausing pattern was dependent on the naked DNA downstream of the nucleosome, we repeated the transcription gel assay shown in Figure 2.5a (shown again in Figure 2.6a for comparison) using a DNA template that lacked a segment downstream of the 601 NPE (Figure 2.6b, upper panel). A very similar pausing pattern was found, both in terms of pausing sites and the 10 bp periodicity, suggesting that the downstream DNA

Figure 2.6. RNAP Pausing Pattern within a Nucleosome is Independent of DNA Downstream of the Nucleosome

(a) RNAP transcribed through a nucleosome in the forward direction of the 601NPE as indicated by the template cartoon (identical to Figure 2.4a). (The same gel as in Figure 2.5a)

(b) RNAP transcribed through a nucleosome in the forward direction of the 601NPE located at the end of the template. Although the 10 bp pausing periodicity was less defined, the pausing positions and the strengths were very similar as in (a). M stands for “10 bp DNA marker”.

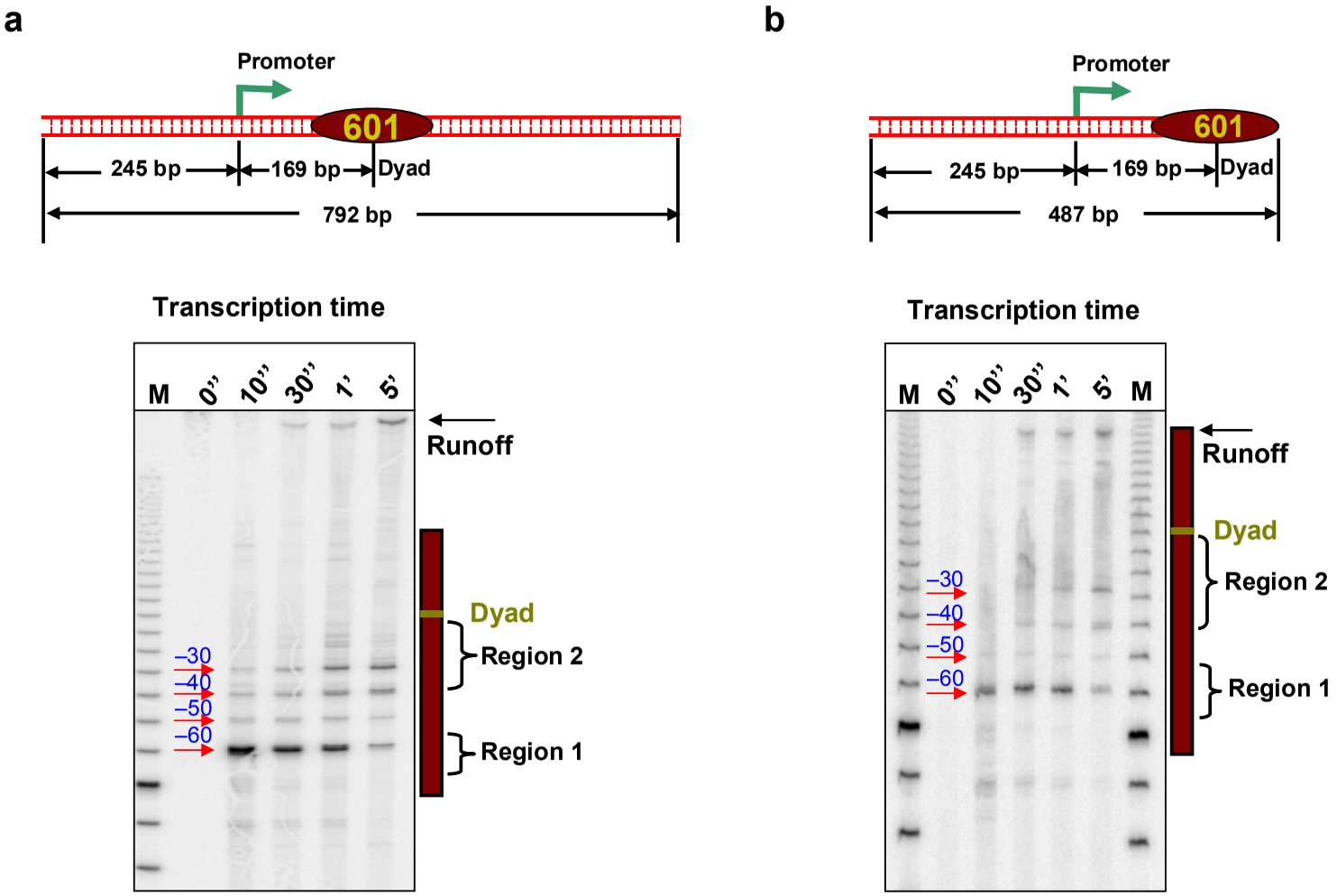
a
Promoter
601
245 bp
169 bp
Dyad
792 bp
Transcription time
M
0''
10''
30''
1'
5'
Runoff
Dyad
Region 2
Region 1
–30
–40
–50
–60
b
Promoter
601
245 bp
169 bp
Dyad
487 bp
Transcription time
M
0''
10''
30''
1'
5'
M
Runoff
Dyad
Region 2
Region 1
–30
–40
–50
–60

was not essential for the pausing pattern. The 10 bp pausing periodicity, however, became less well defined, indicating that the 601 NPE was not able to position a nucleosome as uniquely when it was located at one end of a DNA template.

To examine whether these observations were specific to the DNA sequence transcribed, we placed the promoter on the distal site of the 601NPE and allowed the RNAP to elongation into the nucleosome from the reverse direction (Figure 2.5b). Since the 601NPE sequence is not palindromic, RNAP effectively transcribed a new sequence. We found that all nucleosome-induced pauses were still highlighted by a distinctive 10 bp periodicity. As RNAP encountered histone-DNA interactions, it paused again at around – 60 bp (strong) from the dyad, and then at around – 50 bp (weak), – 40 bp (weak), – 30 bp (strong), and – 20 bp (strong) from the dyad. No strong pauses were detected after the leading edge of RNAP passed the dyad region. The pause patterns from the two sequences are highly similar, indicating that the nucleosome-induced pausing is predominately determined by the strong histone-DNA interactions. The locations of these interactions are specified by the nucleosome structure; and their strengths, to some extent, are regulated by the DNA sequence. Our data suggest that histone-DNA interactions play the most important role in the observed pausing pattern.

Remarkably, these pausing features bear resemblance to the resistance encountered during mechanical unzipping through a nucleosome (Hall et al., 2009). The mechanical experiments revealed that the unzipping fork proceeds smoothly during the initial invasion, pauses at the first off-dyad and dyad

regions of interactions, and again proceeds smoothly through the rest of the nucleosomal DNA with minimal resistance, due to histone dissociation caused by unzipping through the dyad. Although mechanical unzipping encountered resistance with a 5 bp periodicity, we observed that RNAP paused with a 10 bp periodicity. Since the minor groove of the DNA faces the histone core domains roughly every 10 bp, we interpreted the observed 5 bp periodicity during the mechanical unzipping as histone interactions with the two strands of dsDNA at each minor groove (Luger et al., 1997; Hall et al., 2009). The observation that RNAP paused with a 10 bp periodicity suggests that RNAP may cooperatively disrupt a pair of interactions at each DNA minor groove.

RNAP is Backtracked by ~ 10-15 bp upon Encountering a Nucleosome

We investigated the extent of backtracking during nucleosome-induced transcription pausing by comparing the location of the RNAP active site on DNA with the corresponding transcript length. This allowed a direct measurement of the backtracking distance, as compared with conventional methods which typically can only detect transcript length and therefore rely on sensitivity to cleavage factors (TFIIS or GreA/B) for evidence of backtracking.

A line scan of the transcription gel from Figure 2.5a shows that the distribution of the 3' end of RNA peaked at the –60 bp position from the dyad (upon encountering the off-dyad region of interactions) after 10 s of transcription (Figure 2.7b). The corresponding distribution of the location of the RNAP active site, as determined by DNA unzipping, resembles that of the 3' end of RNA, but peaked at –75 bp from the dyad (Figure 2.7c). This clearly shows

Figure 2.7. Histone-DNA Interactions Induce RNAP Backtracking and Prevention of Backtracking Facilitates Transcription

All experiments were conducted using the DNA template shown in Figure 2.4a and for 10 s transcription time. The predominant peak position in each distribution is indicated by an arrow.

(a) A cartoon of a backtracked transcription elongation complex. Pink dashed line indicates the location of the 3' end of RNA, and the purple dashed line indicates the location of RNAP active site.

(b) An intensity scan of the gel shown in Figure 2.5a. The 3' RNA location is specified relative to the dyad.

(c) Distribution of RNAP active site location as determined by the unzipping method. The active site location is specified relative to the dyad. The displacement between the peak location of the active site and that of the 3' end of the RNA indicates the backtracking distance.

(d) Distribution of RNAP active site location in the presence of RNase T1.

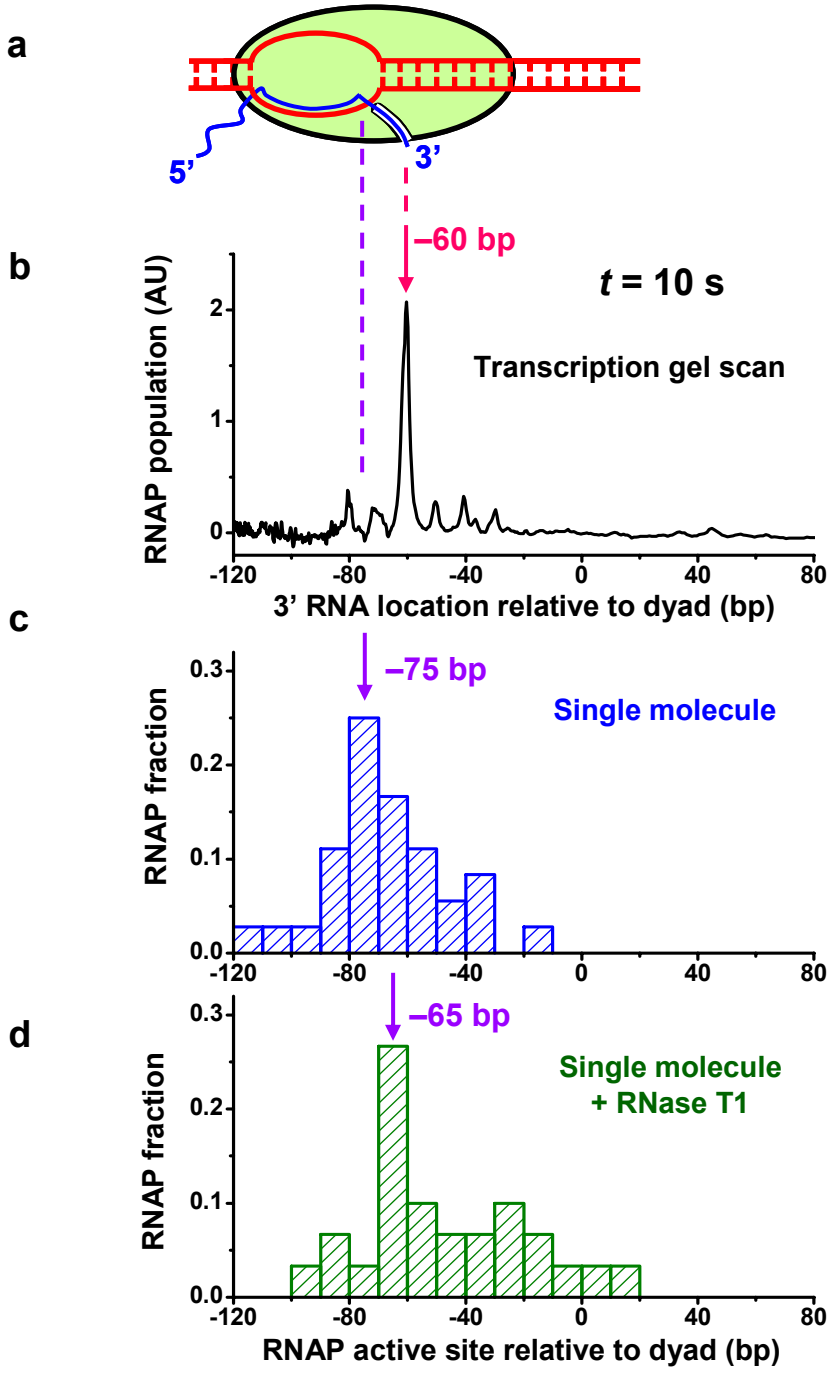
a
5'
3'
b
–60 bp
t = 10 s
Transcription gel scan
RNAP population (AU)
2
1
0
-120
-80
-40
0
40
80
3' RNA location relative to dyad (bp)
c
–75 bp
Single molecule
RNAP fraction
0.3
0.2
0.1
0.0
d
–65 bp
Single molecule
+ RNase T1
RNAP active site relative to dyad (bp)

that a substantial fraction of RNAP was backtracked by ~15 bp during nucleosome-induced pausing (Figure 2.7a). In addition, the active site distribution shows a broader distribution and lacks the 10 bp periodicity, indicating that backtracking occurred over a range of distances at a given pause. After 5 min of transcription, the RNAP progressed further into the nucleosome and encountered the dyad region of strong interactions as indicated by the strong pause sites at –40 bp and –30 bp before the dyad (Figure 2.5a, and Figure 2.6a). RNAP again backtracked with a mean backtracking distance of ~ 10 bp while a small fraction elongated through the nucleosome (Figure 2.8a and b). Compared with the 10 s data, a fraction of RNAP that initially paused continued to elongate, indicating that this fraction was either not backtracked or not backtracked extensively as has been previously reported (Kireeva et al., 2005; Ujvari et al., 2008). However, a substantial fraction was not able to elongate through the nucleosome even after 30 min of transcription (Figure 2.5 and Figure 2.6), indicating that extensive backtracking occurred in this fraction.

To substantiate this conclusion, we conducted an experiment in which RNase T1 was added during the transcription chase reaction (Experimental Procedures) to remove most of the 5' end of the exposed nascent RNA. Since backtracking is only thermodynamically favorable with a full complement of RNA/DNA hybrid, this truncation is expected to facilitate transcription through a nucleosomal template, presumably by limiting the backtracking (Kireeva et al., 2005). Such an effect is difficult to observe using traditional methods that typically measure the length of intact RNA, but the unzipping assay allows direct detection of the RNAP position and thus circumvents this problem. As a

Figure 2.8. 5 Min Transcription Result Obtained from Bulk Transcription Gel Analysis and Single Molecule Unzipping Method

All experiments were conducted using the DNA template shown in Figure 2.4a. The transcription reaction was performed for 5 min. The mean location of each distribution is indicated by a dashed line.

(a) An intensity scan of the gel shown in Figure 2.5a. The 3' RNA location is specified relative to the dyad. The predominant peak positions indicate RNAP pause sites.

(b) Distribution of RNAP active site location as determined by the unzipping method. The active site location is specified relative to the dyad. The displacement between the mean location of the active site and that of the 3' end of the RNA indicates the RNAP backtracking distance.

(c) Distribution of RNAP active site location in the presence of RNase T1.

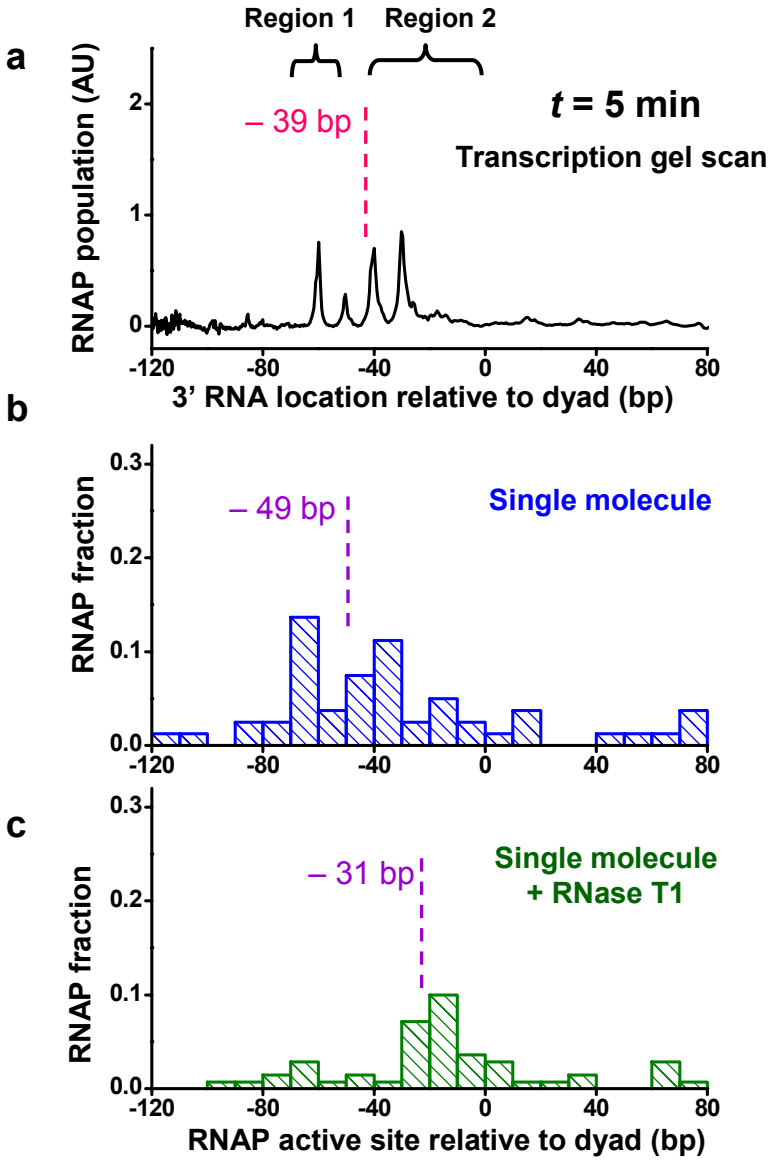
a
Region 1
Region 2
– 39 bp
t = 5 min
Transcription gel scan
RNAP population (AU)
2
1
0
-120
-80
-40
0
40
80
3' RNA location relative to dyad (bp)
b
– 49 bp
Single molecule
RNAP fraction
0.3
0.2
0.1
0.0
c
– 31 bp
Single molecule
+ RNase T1
RNAP active site relative to dyad (bp)

Figure 2.9. RNase T1 does not Alter the Unzipping Force Signature of an RNAP or a Nucleosome

(a) In order to check whether RNase T1 alters RNAP and/or nucleosome unzipping signatures, PTCs were formed on the single promoter nucleosomal templates and the sample was incubated with 5 units/ul RNase T1 at room temperature for 30 min. Unzipping data show unaltered signatures for both a PTC and a nucleosome prior to transcription (black). Unzipping pattern of naked DNA with the same sequence is also shown for comparison (grey).

(b) Transcription was resumed in the presence of RNase T1 and then stopped by EDTA. The histones were subsequently removed by heparin. Representative traces of unzipping through an elongation complex are shown after indicated transcription times, and they show identical unzipping signatures to those in the absence of RNase T1.

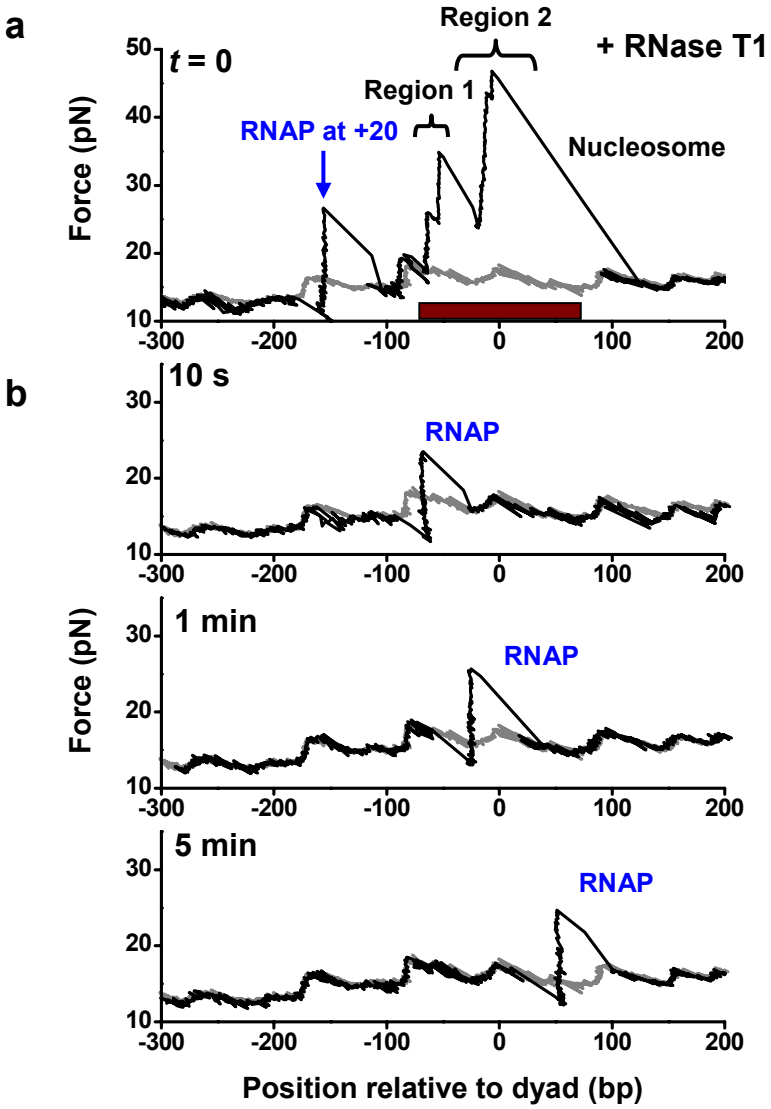
a
b
Region 2
+ RNase T1
t = 0
Region 1
RNAP at +20
Nucleosome
10 s
RNAP
1 min
RNAP
5 min
RNAP
Force (pN)
Force (pN)
Position relative to dyad (bp)

control experiment, we verified that the presence of RNase T1 did not alter the unzipping force signature of the RNAP or the nucleosome (Figure 2.9).

In the presence of RNase T1, after 10 s of transcription, the active site location distribution peaked at −65 bp from the dyad and the peak was better defined (Figure 2.7d). This indicates that when the leading edge of the RNAP encountered the first off-dyad region of interactions in the nucleosome, it still paused but did not significantly backtrack (compare Figures 2.7b, 2.7c, and 2.7d). The reduced backtracking is expected to be less inhibitory to elongation. Consistent with this, a larger fraction of RNAP progressed further downstream (compare Figures 2.7c and 2.7d). After 5 min of transcription, a much smaller population remained on the DNA (compare Figures 2.8b and 2.8c).

Taken together, these results suggest that backtracking is the major cause of nucleosome-induced RNAP pausing and any mechanism that reduces backtracking should facilitate transcription through nucleosomes. These findings are consistent with those from previous studies which suggested that Pol II may undergo backtracking upon encountering a nucleosome (Kireeva et al., 2005). In addition, the current approach provides a quantitative and direct measurement of backtracking distance.

A Trailing RNAP Exerts an Assisting Force on a Leading RNAP to Facilitate Elongation through Nucleosomal DNA

In vivo, the concerted action of multiple RNAPs which elongate in the same direction may facilitate transcription through nucleosomal DNA. A trailing

RNAP may exert an assisting force on a leading RNAP, and thus reduce backtracking of the leading RNAP while facilitating its forward translocation. In order to test this hypothesis, we constructed a DNA template containing two T7A1 promoters, each followed by identical sequences of 36 bp, and both oriented towards a downstream 601 NPE (Figure 2.10a and Figure 2.11a). This was achieved by inserting a second T7A1 promoter upstream of the original one shown in Figure 2.4a. The locations of the two RNAPs were then monitored by the unzipping method which does not suffer from complications caused by overlapping in pause sites from the two RNAPs in a bulk transcription assay.

Using procedures similar to those described for Figures 2.4b and 2.4c, a nucleosome was assembled onto the 601 NPE and then PTCs were formed at both promoters (Experimental Procedures). Transcription was resumed for a specified amount of time by addition of 1 mM NTPs and competitor DNA, and the reaction was quenched by EDTA followed by immediate removal of histones.

First, we examined PTCs that remained near the +20 nt position. Before the NTP chase, unzipping experiments showed clear force signatures for the two RNAPs stalled at their respective +20 nt loci (Figure 2.10b). Upon NTP addition, a majority of the PTCs at each promoter escaped almost instantly (Figure 2.10c). However, a small fraction escaped more slowly and then leveled off with time (Figure 2.10c, inset). For the trailing RNAP, the fraction remaining was clearly backtracked: the more extensive the backtracking, the longer it took for the RNAP to escape (Figure 2.10c and Figure A.3a, dark

Figure 2.10. Trailing RNAP Assists Leading RNAP to Exit an Arrested State

(a) The two-promoter transcription template construct contains two T7A1 promoters followed by a single 601 NPE.

(b) Example unzipping trace from the template shown in (a) containing two PTCs at their respective +20 nt positions. The two RNAPs were detected at their expected locations.

(c) Percentage of RNAP that remained near the +20 nt position versus transcription time for leading and trailing RNAPs. The inset more clearly shows the percentage of the RNAP remaining near the +20 nt.

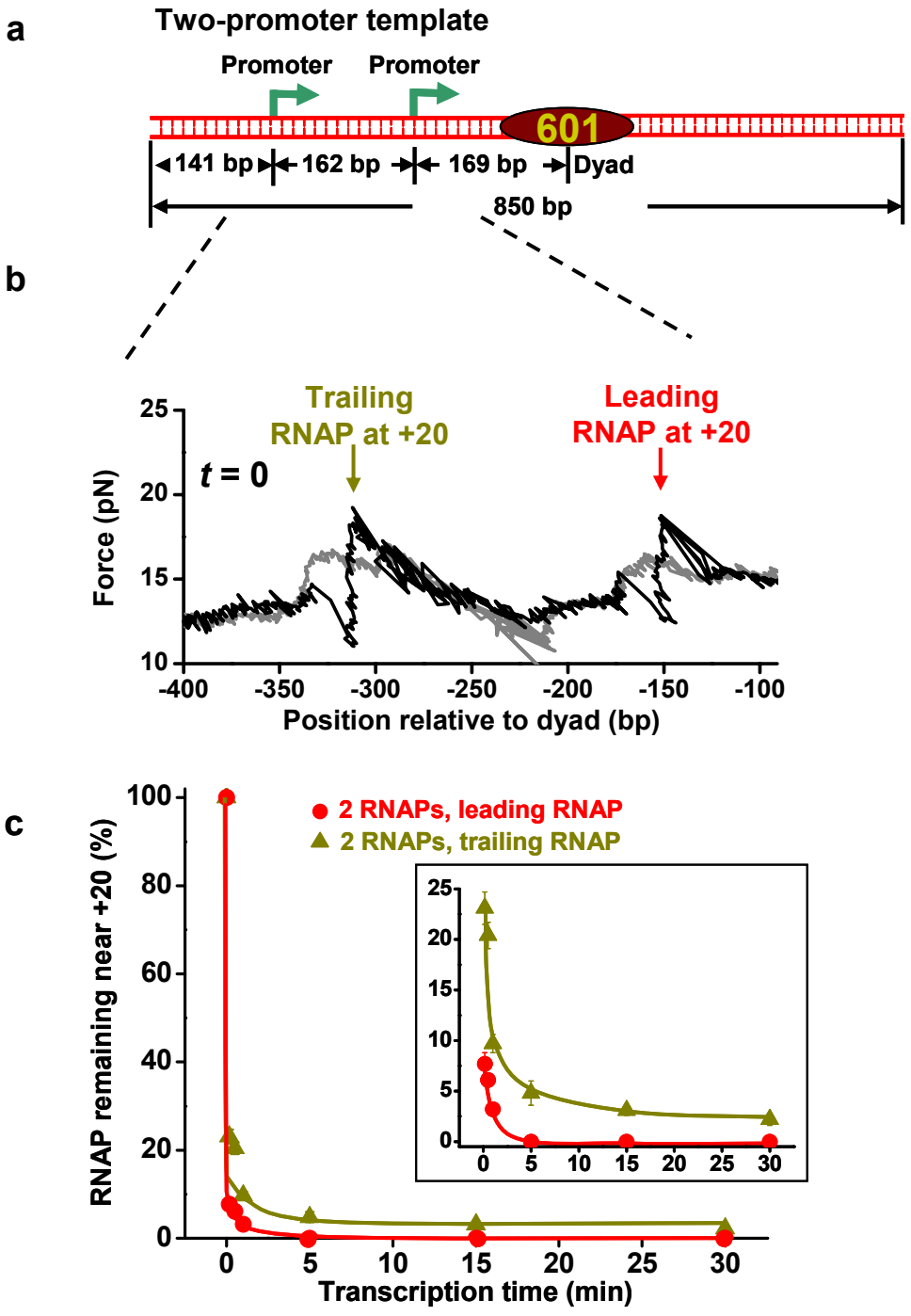
a
Two-promoter template
Promoter
Promoter
601
141 bp
162 bp
169 bp
Dyad
850 bp
b
Trailing
RNAP at +20
Leading
RNAP at +20
t = 0
Force (pN)
25
20
15
10
-400
-350
-300
-250
-200
-150
-100
Position relative to dyad (bp)
c
2 RNAPs, leading RNAP
2 RNAPs, trailing RNAP
RNAP remaining near +20 (%)
100
80
60
40
20
0
0
5
10
15
20
25
30
Transcription time (min)

(yellow). After 30 min of NTP chase, ~ 5% of trailing RNAP remained and they were backtracked by ~ 12 bp. These backtracked complexes were extremely stable and considered arrested on the experimental time scale. These properties were essentially identical to those exhibited by PTCs on the single promoter template (Figure A.3). This result provides direct evidence for nucleosome-independent backtracking. On the other hand, the leading RNAP escaped to completion in $<$ 5 min (Figure 2.10c, red). Given that both PTCs were identical, the different escape behaviors were a result of the interaction between the two RNAPs. This indicates that the trailing RNAP is capable of exerting an assisting force on the leading RNAP to push it out of a backtracked state, rescuing it from an arrested state.

Second, we examined the RNAPs that escaped after NTP addition. Before the NTP chase, unzipping experiments showed clear force signatures for the two RNAPs stalled at their respective +20 nt loci followed by a nucleosome (Figure 2.11b). Figure 2.11c shows representative traces at the resumption of transcription. For each trace, the locations of both RNAPs were clearly discernable. Notice that the two RNAPs were not always found to be in immediate vicinity of each other. While the trailing RNAP would exert a force on the leading RNAP, simultaneously the leading RNAP would exert a reactive force on the trailing RNAP inducing the trailing RNAP to backtrack. Thus a separation could be created between the two RNAPs.

The distribution of the leading RNAP location (Figure 2.11d) showed a resemblance to that of the RNase T1 experiments (Figure 2.7d). Compared

Figure 2.11. Two RNAPs Work Synergistically to Overcome a Nucleosomal Barrier

(a) The two-promoter transcription template construct contains two T7A1 promoters followed by a single 601 NPE (same as Figure 2.10a).

(b) Example unzipping trace from the template shown in (a) containing two PTCs at their respective +20 bp positions and a positioned nucleosome before transcription resumption. The two RNAPs and the nucleosome were detected at their expected locations. The brown bar indicates the 147-bp 601 NPE.

(c) Representative unzipping traces through two elongation complexes on a single DNA molecule after transcription for the indicated durations and removal of histones. Each trace was from a different DNA molecule. Both the leading and trailing RNAPs were detected by their unzipping signatures.

(d) Distribution of the leading RNAP active site location after 10 s transcription reaction.

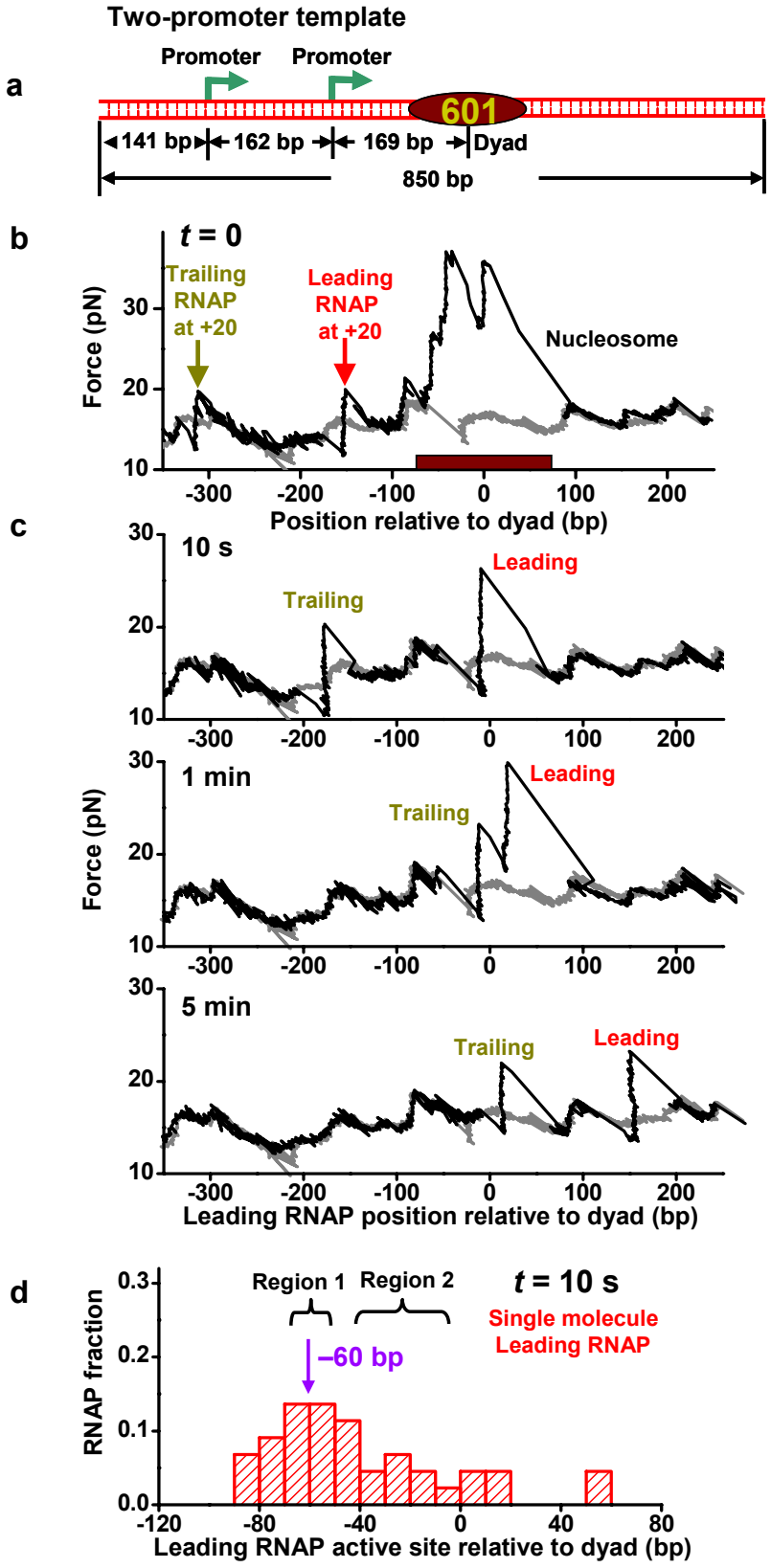
a
Two-promoter template
Promoter
Promoter
601
141 bp
162 bp
169 bp
Dyad
850 bp
b
t = 0
Trailing RNAP at +20
Leading RNAP at +20
Nucleosome
Force (pN)
Position relative to dyad (bp)
c
10 s
Trailing
Leading
1 min
Trailing
Leading
5 min
Trailing
Leading
Force (pN)
Leading RNAP position relative to dyad (bp)
d
Region 1
Region 2
t = 10 s
Single molecule Leading RNAP
–60 bp
RNAP fraction
Leading RNAP active site relative to dyad (bp)

with the single RNAP experiments, the peak location was shifted towards the nucleosome to –60 bp from the dyad with a concurrent increase in the fraction elongating through the nucleosome. Although the leading RNAP still paused upon transcribing to the –60 bp position before the dyad, it did not significantly backtrack.

A Trailing RNAP Enhances the Elongation Rate through a Nucleosome 5-Fold

In order to provide a quantitative measure of elongation rate enhancement of a leading RNAP due to a trailing RNAP, we examined the transcription runoff efficiency of each RNAP as a function of transcription time. Runoff efficiency was computed based on the percentage of DNA templates that showed an absence of RNAP during the DNA unzipping experiments. This computation assumed that an RNAP did not dissociate until it reached the runoff end. Several lines of evidence support this assumption. First, in the single RNAP experiments, we examined the runoff efficiency versus time from the transcription gel and compared it with the corresponding fraction of the DNA templates that showed an absence of an RNAP (Figure 2.12a). The two curves were essentially identical, indicating that no RNAP dissociated before the runoff end. This finding was also supported by previous studies that separately assayed RNA associated with, versus released from, a DNA template (Kireeva et al., 2002). In those studies, the released RNA, resulting from RNAP dissociation, was only full-length transcript. Previous studies also showed that front-to-back collision between two *E. coli* RNAPs did not induce RNAP dissociation (Toulme et al., 1999).

Figure 2.12. Transcription Efficiency Comparison

(a) RNAP runoff and dissociation from the DNA template as a function of transcription time. The runoff percentage was determined from the transcription gel shown in Figure 2.5a. The naked DNA percentage was determined from single molecule experiments such as those shown in Figures 2.4c. The excellent agreement between these data indicates that RNAP only dissociated at the runoff end.

(b) Transcription runoff efficiencies vs. transcription time. A runoff efficiency was represented by the percentage of DNA template that showed an absence of RNAP during DNA unzipping experiments. The error bars are standard errors of the means. Smooth curves passing through the data points for each transcription condition were drawn for ease of comparison (not fits). Naked DNA runoff efficiency (black) was obtained from PAGE gel analysis and is shown for comparison.

(c) Bar plot of relative transcription rates through nucleosomal DNA. The rate of a single RNAP transcribing through a nucleosomal template is used as a reference. The initial rates were estimated from the slopes of linear fits to the near zero transcription times ($\leq$ 1 min).

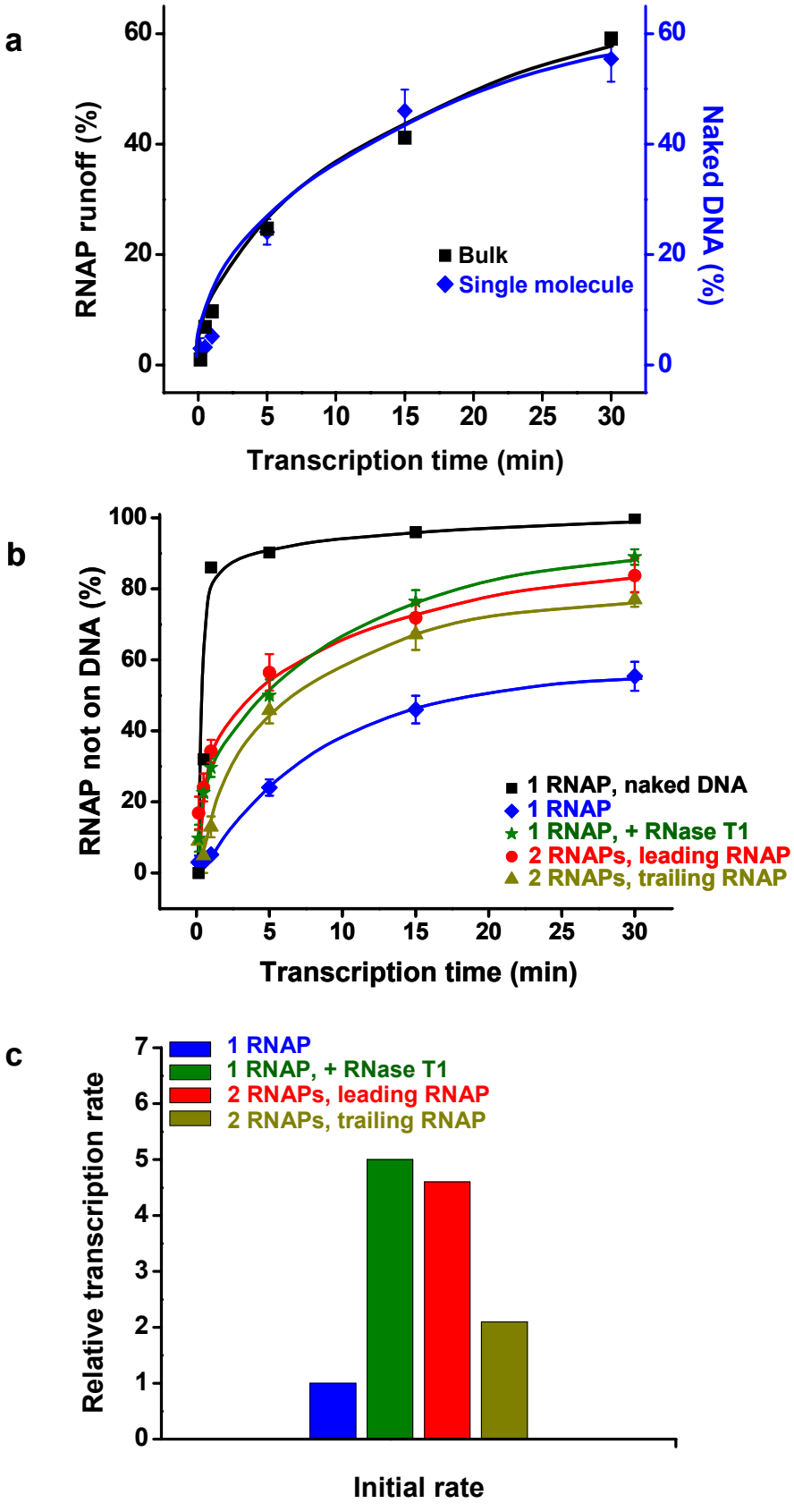
a
RNAP runoff (%)
Naked DNA (%)
Transcription time (min)
Bulk
Single molecule
b
RNAP not on DNA (%)
Transcription time (min)
1 RNAP, naked DNA
1 RNAP
1 RNAP, + RNase T1
2 RNAPs, leading RNAP
2 RNAPs, trailing RNAP
c
Relative transcription rate
Initial rate
1 RNAP
1 RNAP, + RNase T1
2 RNAPs, leading RNAP
2 RNAPs, trailing RNAP

Figure 2.12b shows transcription runoff efficiency versus transcription time. In order to accurately compute this fraction, we corrected for two small but significant contributions: templates without a nucleosome at the 601 NPE or without PTC formation (see Appendix Discussion). The runoff efficiencies are more concisely summarized in Figure 2.12c, in which the initial transcription rate near zero transcription times were used to quantify the comparison. When a single RNAP transcribed through a mononucleosomal template of ~ 550 bp total transcript size, the transcription rate was reduced ~ 20 fold relative to that of naked DNA. However, this rate was increased ~ 5-fold with the assistance of a trailing RNAP, a rate enhancement comparable to that achieved by using RNase T1. Even the trailing RNAP showed a ~ 2 fold rate enhancement compared with that from a single RNAP alone. This is consistent with at least partial eviction of histones by the leading RNAP as evidenced by the lack of pausing sites after RNAP moved beyond the dyad region of interactions (Figure 2.5 and Figure 2.6).

Transcription through a Nucleosome Leads to Histone Loss

When an RNAP encounters a nucleosome, what happens to the histones? In vitro studies suggest that Pol III is able to transfer histones upstream of the original location of the nucleosome, presumably via a transient loop formation mechanism (Studitsky et al., 1995; Studitsky et al., 1997; Bednar et al., 1999). Although the fate of a nucleosome after transcription is largely unresolved for Pol II, studies so far suggest that there may be at least partial, if not complete, loss of histones. Under elevated salt conditions, transcription through a nucleosome by either Pol II or *E. coil* RNAP has been shown to lead to a loss

of one copy of H2A/H2B dimer, leaving behind a hexasome at the original location of the nucleosome in vitro (Kireeva et al., 2002; Walter et al., 2003). Interestingly in vivo studies of Pol II transcription show that nucleosomes are depleted in regions of highly transcribed genes (Kristjuhan and Svejstrup, 2004; Lee et al., 2004).

We conducted experiments to investigate the fate of histones after transcription. Several scenarios are possible involving both the locations and types of histones that remain on the DNA. The histones may remain at their original location, be relocated, or completely dissociate from the DNA. Any remaining histones may form an octamer, or incur loss of some histones. To distinguish among these possibilities, a real-time transcription experiment was carried out with DNA unzipping. In contrast to the aforementioned experiments, the transcription reaction was not quenched and nor was heparin added to dissociate the histones. The locations of bound proteins were then determined while the transcription was taking place over a nucleosomal DNA. These real-time assays avoided histone dissociation or nucleosome structural re-arrangements that were unrelated to transcription. These experiments were conducted using a template shown in Figure 2.4a that contained a single promoter and a positioned nucleosome.

As a control experiment, the location of a positioned nucleosome was examined prior to PTC formation. As the DNA was unzipped through a nucleosome, the first force rise that was significantly above the baseline was located, as expected, at −60 bp from the dyad at the beginning of the first off-

Figure 2.13. Histone Fates upon Transcription Obtained From Real Time Transcription Experiments

All experiments were conducted using the single promoter DNA template shown in Figure 2.4a.

(a) Percentage of DNA templates with bound protein vs. transcription time. The real-time experiments (red) detected the percentage of the templates with bound RNAP and/or histones. For comparison, the corresponding percentage with bound RNAP (blue) was also plotted based on Figure 2.12b (blue, 1 RNAP data). Smooth curves passing through each set of data points were drawn for ease of comparison (not fits).

(b) Distributions of bound protein (RNAP or histone) location upon transcription as determined by the first force rise during the real-time experiments. Each distribution contained 46-73 measurements. For comparison, the distribution of the location of bound histones before NTP addition (grey) was also plotted.

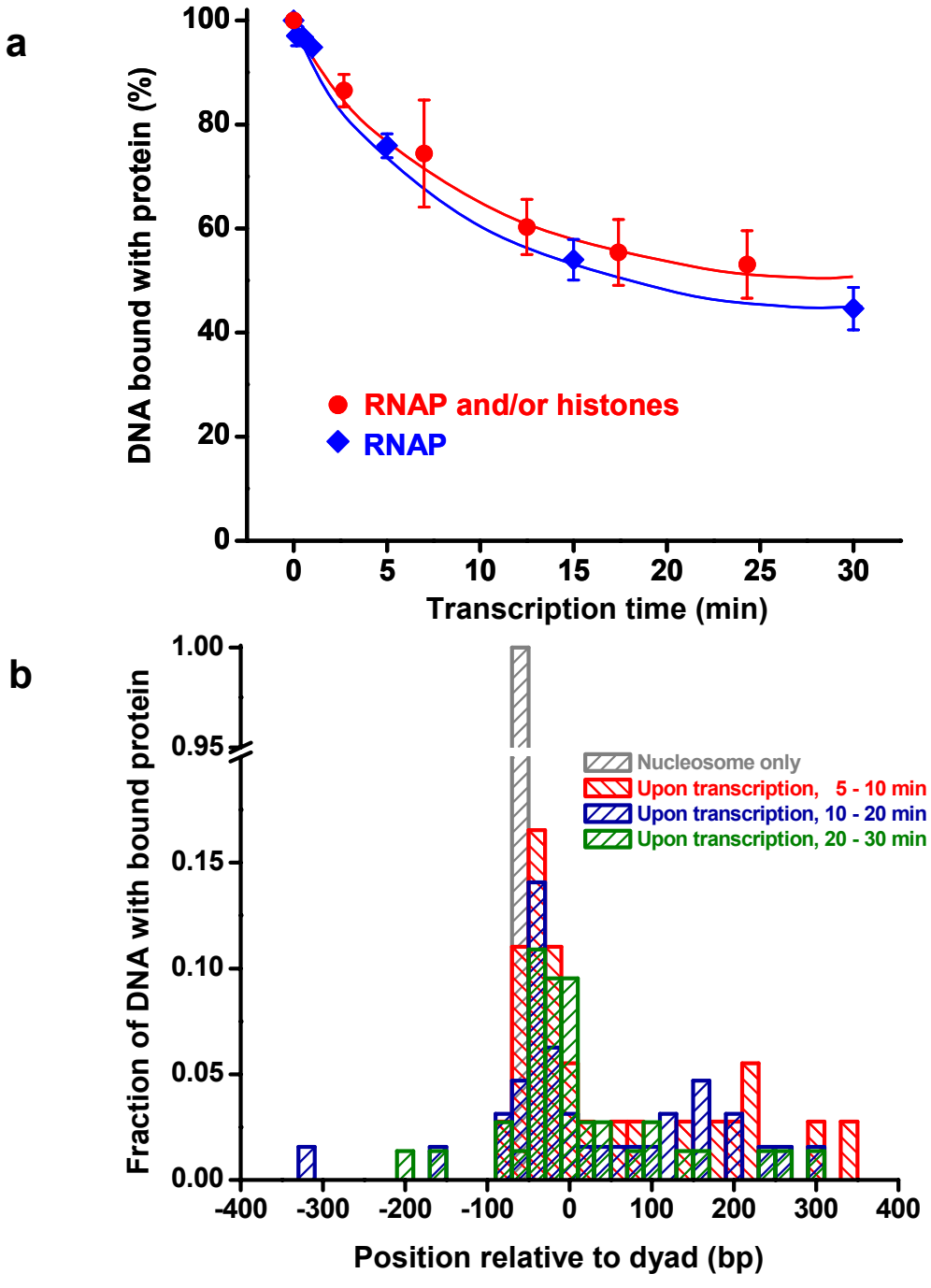
a
DNA bound with protein (%)
100
80
60
40
20
0
0
5
10
15
20
25
30
Transcription time (min)
RNAP and/or histones
RNAP
b
Fraction of DNA with bound protein
1.00
0.95
0.15
0.10
0.05
0.00
-400
-300
-200
-100
0
100
200
300
400
Position relative to dyad (bp)
Nucleosome only
Upon transcription, 5 - 10 min
Upon transcription, 10 - 20 min
Upon transcription, 20 - 30 min

dyad region of strong histone-DNA interactions in a nucleosome (Figure 2.13b, grey).

To begin the real-time experiment, a PTC was formed on the nucleosomal DNA and transcription was resumed by an addition of 1 mM NTPs along with competitor DNA into the single molecule sample chamber. The added competitor DNA prevented re-initiation but did not alter transcription through a nucleosome (Figure A.1 legend). Each DNA template was rapidly unzipped while RNAP transcribed through the nucleosome to locate the first force rise. Because both RNAP and histones might be present, unzipping force signatures were variable and a detected force rise location might be indicative of either an RNAP or bound histones (for example traces, see Figure 2.14b).

Several lines of evidence suggest that histone dissociation was predominant upon transcription. First, at a given transcription time, a significant fraction of the templates showed a force signature consistent with that of naked DNA (Figure 2.13a). This fraction increased with time. At 30 min, ~ 50% of the templates were naked DNA. Thus at least for this fraction, histones were evicted from the DNA upon transcription. Second, at a given time, the fraction of DNA templates that contained RNAP and/or histones (Figure 2.13a, red curve) was only slightly higher than that containing RNAP (converted from Figure 2.12b, blue curve). Therefore, for most templates, histones were only present on a DNA template when an RNAP was present, and RNAP runoff led to complete histone dissociation. The difference between these two curves

Figure 2.14. Unzipping Traces When RNAP is in the Vicinity of the Histones

(a) When RNAP and histones are separated, their unzipping signatures are clearly distinguishable (black). Unzipping through a naked DNA with the same sequence is shown for comparison (grey).

(b) When RNAP is in the vicinity of the histones, their individual unzipping signatures are undifferentiable. Representative traces (magenta, blue) were selected from real-time transcription experiment. The transcription durations are indicated. Unzipping through a naked DNA with the same sequence is shown for comparison (grey).

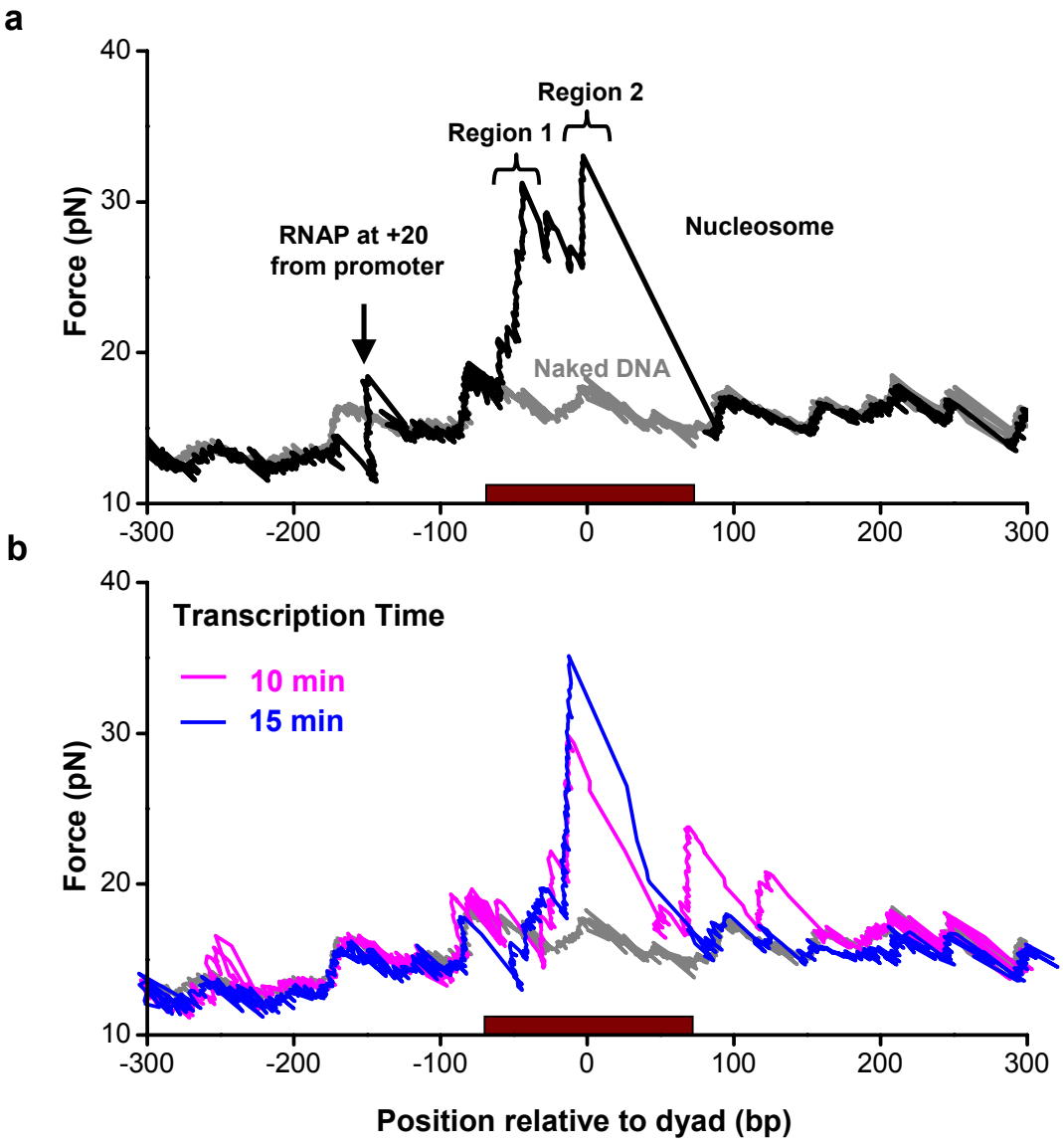
a
40
30
20
10
Force (pN)
Region 2
Region 1
RNAP at +20
from promoter
Nucleosome
Naked DNA
-300
-200
-100
0
100
200
300
b
Transcription Time
10 min
15 min
Position relative to dyad (bp)

was small (~ 5% at 30 min) and may represent a small fraction of the templates that contained histones after RNAP runoff. Third, the distribution for the locations of the first force peak shifted progressively downstream with time, as would be expected if the force rise was detecting RNAP. The distribution for data from 5-10 min (Figure 2.13b) resembled that of the RNAP distribution at 5 min (Figure 2.7c). Fourth, the vast majority of the first force rises detected were located downstream of the nucleosome force rise prior to transcription. This indicates that RNAP did not relocate histones upstream of the original nucleosome. The upstream translocation of histones, if it exists, is a minor mechanism.

DISCUSSION

In eukaryotic cells, DNA is tightly packed into nucleosomes which are known to be major barriers to transcription. At the same time, cells have developed various mechanisms to allow efficient passage of RNAP through nucleosomes. In this study, we used a simplified model system comprised of *E. coli* RNAP and a positioned nucleosome to investigate the mechanism of nucleosome-induced RNAP pausing/arrest, and whether and how multiple RNAPs on the same nucleosomal DNA could work synergistically to overcome the nucleosome barrier during transcription. This was achieved by single molecule DNA unzipping techniques in conjunction with bulk transcription studies.

This work provides a coherent picture of transcription through a nucleosome (Figure 2.15). As an RNAP encounters a nucleosome barrier, it must sequentially overcome the histone-DNA interactions within the nucleosome. The locations and strengths of these interactions dictate the pausing pattern of the RNAP, yielding pausing behaviors that are characteristic of these interactions. Pauses occur approximately every 10 bp (when RNAP encounters DNA minor groove interactions with the core histone surface), with the strongest pausing at around −60 bp before the dyad (upon encountering the first off-dyad region of strong interactions) and at around −30 bp before the dyad (upon encountering the dyad region of strong interactions), but no pausing occurs once the leading edge of the RNAP passes the dyad region (possibly due to histone dissociation). At each pause site prior to reaching the dyad region, RNAP may backtrack to a variable distance and the mean backtracking distance is ~ 10-15 bp. Such a large backtracking distance makes it difficult for RNAP to resume active elongation. Thus any mechanism that would reduce backtracking should facilitate the escape of RNAP from a nucleosome-induced backtracking pause. A trailing RNAP, which initiates from the same or a different promoter, may then catch up with a leading RNAP and exert an assisting force on it to facilitate its exit from the backtracked state and entry into productive elongation. Once the leading RNAP overcomes the dyad region of interactions, it may then proceed forward with little resistance.

The Nature of the Nucleosome Barrier

The current work employed *E. coli* RNAP but many findings here may also be more generally applicable to Pol II. Our work provides a new interpretation of

Figure 2.15. Cartoon Illustrating the Mechanism of Transcription through Nucleosomal DNA

As an RNAP approaches a nucleosome (a), it encounters histone-DNA interactions in a nucleosome which induce RNAP pausing and likely backtracking (b). The arrival of a trailing RNAP (c) exerts an assisting force on the leading RNAP (d), rescuing the leading RNAP from its backtracked state. The two RNAPs, working synergistically, eventually evict downstream histones, resulting in the removal of the nucleosomal barrier and efficient transcription (e). Regions of strong histone-DNA interactions in the nucleosomal DNA are indicated in red.

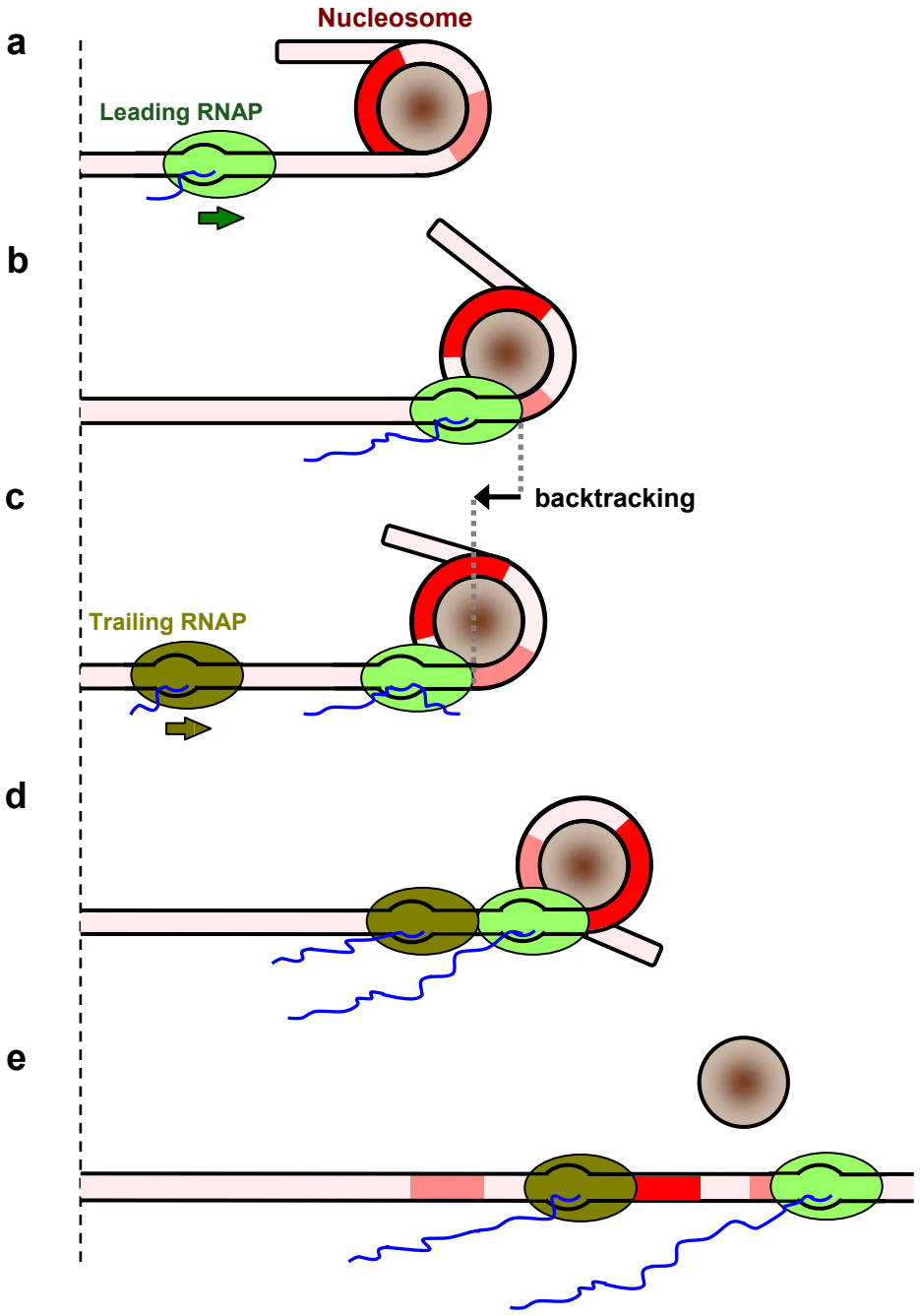
a
Nucleosome
Leading RNAP
b
c
backtracking
Trailing RNAP
d
e

the nature of the transcription pausing pattern at a nucleosome and suggests the importance of the strengths and locations of histone-DNA interactions within a nucleosome in dictating pausing behavior. In light of this interpretation, the current work needs to be placed in the context of previous work and some conclusions from previous work also should be re-examined.

First, we showed that *E. coli* RNAP displayed a characteristic 10 bp periodic pausing pattern when encountering the promoter-proximal half of the nucleosome. Such periodicity has not been explicitly reported for Pol II or *E. coli* RNAP and the apparent lack of reported periodicity may be due to nucleosome positioning heterogeneity. In previous studies, a mononucleosome was positioned using either a 5s RNA NPE (Kireeva et al., 2002; Walter et al., 2003; Kireeva et al., 2005), or 601 and 603 NPEs (Bondarenko et al., 2006; Ujvari et al., 2008). It is well known that the 5s rRNA NPE generates several major and minor nucleosome positions (Dong et al., 1990) and nucleosome-specific pauses might have been masked by multiple sequence-specific pause sites enhanced by the presence of nucleosome. We also found that even the 601 NPE was not able to position a nucleosome as uniquely when it was located at one end of a DNA template as opposed to when it was located near the center of a DNA template flanked by long stretches of DNA (Figure 2.6). The ability of the 601 NPE to position a nucleosome may even be less unique for short DNA templates, which were employed in previous biochemistry studies, containing a nucleosome necessarily near both ends of the DNA (Bondarenko et al., 2006).

Nonetheless there have been interesting hints of the presence of a 10 bp pausing periodicity of Pol II from those previous studies. A careful inspection of data from Bondarenko et al. and Ujvari et al. reveals that Pol II in fact paused roughly with a 10-bp periodicity on a template containing either a 603 NPE or a 601R NPE positioned nucleosome (Bondarenko et al., 2006; Ujvari et al., 2008). Also, the 10 bp pausing periodicity was observed for Pol III (Studitsky et al., 1997) but was interpreted as a restricted rotation of Pol III due to DNA loop formation. Our work offers an alternative and much simpler explanation.

Second, we found that the strongest pause sites occurred at around −60 bp (strong), and then −30 bp before the dyad. Essentially identical pausing regions were identified for Pol II albeit with a lack of distinct, or less pronounced, periodicity (Kireeva et al., 2005; Bondarenko et al., 2006; Ujvari et al., 2008). This again suggests a high degree of similarity in the nature of the nucleosome barrier encountered by *E. coil* RNAP and Pol II as has been previously reported (Walter et al., 2003).

Third, we have provided direct evidence for *E. coli* RNAP backtracking upon encountering a nucleosome barrier and show that the mean backtracking distance is ~ 10-15 bp. This finding is entirely consistent with previous work that showed cleavage sensitivity of transcripts to TFIIS for Pol II (Kireeva et al., 2005). Our finding that RNase T1 can facilitate transcription through a nucleosome is also consistent with these studies. The current work, however, has provided a more direct method to quantitatively determine the extent of backtracking.

Implications for Transcription in Vivo

In this work, we have provided direct evidence for the synergistic actions of multiple RNAPs working in concert to overcome the nucleosome barrier. In the presence of a trailing RNAP, a leading RNAP was found to transcribe through a nucleosome with a 5-fold rate enhancement. The trailing RNAP is capable of exerting an assisting force on the leading RNAP and facilitating the leading RNAP to exit the backtracked state and resume elongation. Indeed RNAPs are known to be powerful molecular motors that can exert forces and work against resistance. *E. coli* RNAP is able to generate ~ 27 pN of force (Wang et al., 1998), and Pol II at least ~ 8 pN of force (Galburt et al., 2007). Forces of such magnitude have been shown to significantly speed active elongation rates on naked DNA (Shaevitz et al., 2003; Bai et al., 2007).

In vivo, multiple initiation is common among highly expressed genes. It has been demonstrated that the rates and efficiencies of transcription elongation in various eukaryotic and prokaryotic cells are directly proportional to the rates of transcriptional initiation (Yankulov et al., 1994; Epshtein et al., 2003). Although transcription elongation factors have been found to associate with coding regions in vivo, there is also evidence that many transcription factors that travel along with Pol II, do not affect the Pol II elongation rate (Mason and Struhl, 2005; Schwabish and Struhl, 2007). Remarkably, cleavage factors, that have been suggested to reactivate backtracked RNAP and contribute to the rapid progression of RNAP elongation, are dispensable in vivo under physiological conditions (Archambault et al., 1992; Orlova et al., 1995). Therefore, it is likely that multiple initiation may serve as an alternative

mechanism to remove roadblocks, such as nucleosomes and other DNA binding proteins, during transcription.

It has recently been suggested that during multiple initiation the leading RNAP that first encounters nucleosomes might be a specialized “pioneer” polymerase equipped with additional factors to open unmodified, fully repressed chromatin (Orphanides and Reinberg, 2000). However there is little evidence that such a pioneer RNAP differs from its trailing RNAPs. Then how does a pioneer RNAP work so effectively? Our study suggests a much simpler explanation without invoking a pioneer RNAP of unique properties. The initial few RNAPs may together function as a group effectively acting as pioneer RNAPs so that their additive force is sufficient to evict histones and thereby establish a more accessible chromatin for trailing RNAPs.

REFERENCES

Anderson, J.D., Lowary, P.T., and Widom, J. (2001). Effects of histone acetylation on the equilibrium accessibility of nucleosomal DNA target sites. J Mol Biol *307*, 977-985.

Archambault, J., Lacroute, F., Ruet, A., and Friesen, J.D. (1992). Genetic interaction between transcription elongation factor TFIIS and RNA polymerase II. Mol Cell Biol *12*, 4142-4152.

Awrey, D.E., Shimasaki, N., Koth, C., Weilbaecher, R., Olmsted, V., Kazanis, S., Shan, X., Arellano, J., Arrowsmith, C.H., Kane, C.M.*, et al.* (1998). Yeast transcript elongation factor (TFIIS), structure and function. II: RNA polymerase binding, transcript cleavage, and read-through. J Biol Chem *273*, 22595-22605.

Bai, L., Fulbright, R.M., and Wang, M.D. (2007). Mechanochemical kinetics of transcription elongation. Phys Rev Lett *98*, 068103.

Balandina, A., Kamashev, D., and Rouviere-Yaniv, J. (2002). The bacterial histone-like protein HU specifically recognizes similar structures in all nucleic acids. DNA, RNA, and their hybrids. J Biol Chem *277*, 27622-27628.

Bednar, J., Studitsky, V.M., Grigoryev, S.A., Felsenfeld, G., and Woodcock, C.L. (1999). The nature of the nucleosomal barrier to transcription: direct observation of paused intermediates by electron cryomicroscopy. Mol Cell *4*, 377-386.

Belotserkovskaya, R., Oh, S., Bondarenko, V.A., Orphanides, G., Studitsky, V.M., and Reinberg, D. (2003). FACT facilitates transcription-dependent nucleosome alteration. Science *301*, 1090-1093.

Bondarenko, V.A., Steele, L.M., Ujvari, A., Gaykalova, D.A., Kulaeva, O.I., Polikanov, Y.S., Luse, D.S., and Studitsky, V.M. (2006). Nucleosomes can form a polar barrier to transcript elongation by RNA polymerase II. Mol Cell *24*, 469-479.

Brown, C.E., Lechner, T., Howe, L., and Workman, J.L. (2000). The many HATs of transcription coactivators. Trends Biochem Sci *25*, 15-19.

Darzacq, X., Shav-Tal, Y., de Turris, V., Brody, Y., Shenoy, S.M., Phair, R.D., and Singer, R.H. (2007). In vivo dynamics of RNA polymerase II transcription. Nat Struct Mol Biol *14*, 796-806.

Dong, F., Hansen, J.C., and van Holde, K.E. (1990). DNA and protein determinants of nucleosome positioning on sea urchin 5S rRNA gene sequences in vitro. Proc Natl Acad Sci U S A *87*, 5724-5728.

Ebright, R.H. (2000). RNA polymerase: structural similarities between bacterial RNA polymerase and eukaryotic RNA polymerase II. J Mol Biol *304*, 687-698.

Epshtein, V., Toulme, F., Rahmouni, A.R., Borukhov, S., and Nudler, E. (2003). Transcription through the roadblocks: the role of RNA polymerase cooperation. EMBO J *22*, 4719-4727.

Galburt, E.A., Grill, S.W., Wiedmann, A., Lubkowska, L., Choy, J., Nogales, E., Kashlev, M., and Bustamante, C. (2007). Backtracking determines the force sensitivity of RNAP II in a factor-dependent manner. Nature *446*, 820-823.

Hall, M.A., Shundrovsky, A., Bai, L., Fulbright, R.M., Lis, J.T., and Wang, M.D. (2009). High-resolution dynamic mapping of histone-DNA interactions in a nucleosome. Nat Struct Mol Biol *16*, 124-129.

Izban, M.G., and Luse, D.S. (1991). Transcription on nucleosomal templates by RNA polymerase II in vitro: inhibition of elongation with enhancement of sequence-specific pausing. Genes Dev *5*, 683-696.

Kireeva, M.L., Hancock, B., Cremona, G.H., Walter, W., Studitsky, V.M., and Kashlev, M. (2005). Nature of the nucleosomal barrier to RNA polymerase II. Mol Cell *18*, 97-108.

Kireeva, M.L., Walter, W., Tchernajenko, V., Bondarenko, V., Kashlev, M., and Studitsky, V.M. (2002). Nucleosome remodeling induced by RNA polymerase II: loss of the H2A/H2B dimer during transcription. Mol Cell *9*, 541-552.

Koch, S.J., Shundrovsky, A., Jantzen, B.C., and Wang, M.D. (2002). Probing protein-DNA interactions by unzipping a single DNA double helix. Biophys J *83*, 1098-1105.

Komissarova, N., and Kashlev, M. (1997). Transcriptional arrest: Escherichia coli RNA polymerase translocates backward, leaving the 3' end of the RNA intact and extruded. Proc Natl Acad Sci U S A *94*, 1755-1760.

Korzheva, N., and Mustaev, A. (2001). Transcription elongation complex: structure and function. Curr Opin Microbiol *4*, 119-125.

Korzheva, N., Mustaev, A., Kozlov, M., Malhotra, A., Nikiforov, V., Goldfarb, A., and Darst, S.A. (2000). A structural model of transcription elongation. Science *289*, 619-625.

Kristjuhan, A., and Svejstrup, J.Q. (2004). Evidence for distinct mechanisms facilitating transcript elongation through chromatin in vivo. EMBO J *23*, 4243-4252.

Lathe, R., Buc, H., Lecocq, J.P., and Bautz, E.K. (1980). Prokaryotic histone-like protein interacting with RNA polymerase. Proc Natl Acad Sci U S A *77*, 3548-3552.

Lee, C.K., Shibata, Y., Rao, B., Strahl, B.D., and Lieb, J.D. (2004). Evidence for nucleosome depletion at active regulatory regions genome-wide. Nat Genet *36*, 900-905.

Lee, D.N., and Landick, R. (1992). Structure of RNA and DNA chains in paused transcription complexes containing Escherichia coli RNA polymerase. J Mol Biol *228*, 759-777.

Lowary, P.T., and Widom, J. (1998). New DNA sequence rules for high affinity binding to histone octamer and sequence-directed nucleosome positioning. J Mol Biol *276*, 19-42.

Luger, K., Mader, A.W., Richmond, R.K., Sargent, D.F., and Richmond, T.J. (1997). Crystal structure of the nucleosome core particle at 2.8 A resolution. Nature *389*, 251-260.

Mason, P.B., and Struhl, K. (2005). Distinction and relationship between elongation rate and processivity of RNA polymerase II in vivo. Mol Cell *17*, 831-840.

Nudler, E., Gusarov, I., Avetissova, E., Kozlov, M., and Goldfarb, A. (1998). Spatial organization of transcription elongation complex in Escherichia coli. Science *281*, 424-428.

O'Brien, T., and Lis, J.T. (1993). Rapid changes in Drosophila transcription after an instantaneous heat shock. Mol Cell Biol *13*, 3456-3463.

Orlova, M., Newlands, J., Das, A., Goldfarb, A., and Borukhov, S. (1995). Intrinsic transcript cleavage activity of RNA polymerase. Proc Natl Acad Sci U S A *92*, 4596-4600.

Orphanides, G., and Reinberg, D. (2000). RNA polymerase II elongation through chromatin. Nature *407*, 471-475.

Pal, M., Ponticelli, A.S., and Luse, D.S. (2005). The role of the transcription bubble and TFIIB in promoter clearance by RNA polymerase II. Mol Cell *19*, 101-110.

Roth, S.Y., Denu, J.M., and Allis, C.D. (2001). Histone acetyltransferases. Annu Rev Biochem *70*, 81-120.

Samkurashvili, I., and Luse, D.S. (1996). Translocation and transcriptional arrest during transcript elongation by RNA polymerase II. J Biol Chem *271*, 23495-23505.

Schwabish, M.A., and Struhl, K. (2007). The Swi/Snf complex is important for histone eviction during transcriptional activation and RNA polymerase II elongation in vivo. Mol Cell Biol *27*, 6987-6995.

Shaevitz, J.W., Abbondanzieri, E.A., Landick, R., and Block, S.M. (2003). Backtracking by single RNA polymerase molecules observed at near-base-pair resolution. Nature *426*, 684-687.

Shundrovsky, A., Santangelo, T.J., Roberts, J.W., and Wang, M.D. (2004). A single-molecule technique to study sequence-dependent transcription pausing. Biophys J *87*, 3945-3953.

Shundrovsky, A., Smith, C.L., Lis, J.T., Peterson, C.L., and Wang, M.D. (2006). Probing SWI/SNF remodeling of the nucleosome by unzipping single DNA molecules. Nat Struct Mol Biol *13*, 549-554.

Studitsky, V.M., Clark, D.J., and Felsenfeld, G. (1995). Overcoming a nucleosomal barrier to transcription. Cell *83*, 19-27.

Studitsky, V.M., Kassavetis, G.A., Geiduschek, E.P., and Felsenfeld, G. (1997). Mechanism of transcription through the nucleosome by eukaryotic RNA polymerase. Science *278*, 1960-1963.

Tennyson, C.N., Klamut, H.J., and Worton, R.G. (1995). The human dystrophin gene requires 16 hours to be transcribed and is cotranscriptionally spliced. Nat Genet *9*, 184-190.

Toulme, F., Guerin, M., Robichon, N., Leng, M., and Rahmouni, A.R. (1999). In vivo evidence for back and forth oscillations of the transcription elongation complex. EMBO J *18*, 5052-5060.

Toulme, F., Mosrin-Huaman, C., Artsimovitch, I., and Rahmouni, A.R. (2005). Transcriptional pausing in vivo: a nascent RNA hairpin restricts lateral movements of RNA polymerase in both forward and reverse directions. J Mol Biol *351*, 39-51.

Toulme, F., Mosrin-Huaman, C., Sparkowski, J., Das, A., Leng, M., and Rahmouni, A.R. (2000). GreA and GreB proteins revive backtracked RNA polymerase in vivo by promoting transcript trimming. EMBO J *19*, 6853-6859.

Ujvari, A., Hsieh, F.K., Luse, S.W., Studitsky, V.M., and Luse, D.S. (2008). Histone N-terminal tails interfere with nucleosome traversal by RNA polymerase II. J Biol Chem *283*, 32236-32243.

Varv, S., Kristjuhan, K., and Kristjuhan, A. (2007). RNA polymerase II determines the area of nucleosome loss in transcribed gene loci. Biochem Biophys Res Commun *358*, 666-671.

Walter, W., Kireeva, M.L., Studitsky, V.M., and Kashlev, M. (2003). Bacterial polymerase and yeast polymerase II use similar mechanisms for transcription through nucleosomes. J Biol Chem *278*, 36148-36156.

Walter, W., and Studitsky, V.M. (2001). Facilitated transcription through the nucleosome at high ionic strength occurs via a histone octamer transfer mechanism. J Biol Chem *276*, 29104-29110.

Wang, M.D., Schnitzer, M.J., Yin, H., Landick, R., Gelles, J., and Block, S.M. (1998). Force and velocity measured for single molecules of RNA polymerase. Science *282*, 902-907.

Weilbaecher, R.G., Awrey, D.E., Edwards, A.M., and Kane, C.M. (2003). Intrinsic transcript cleavage in yeast RNA polymerase II elongation complexes. J Biol Chem *278*, 24189-24199.

Widom, J. (2001). Role of DNA sequence in nucleosome stability and dynamics. Q Rev Biophys *34*, 269-324.

Yankulov, K., Blau, J., Purton, T., Roberts, S., and Bentley, D.L. (1994). Transcriptional elongation by RNA polymerase II is stimulated by transactivators. Cell *77*, 749-759.

Zaychikov, E., Denissova, L., and Heumann, H. (1995). Translocation of the Escherichia coli transcription complex observed in the registers 11 to 20: "jumping" of RNA polymerase and asymmetric expansion and contraction of the "transcription bubble". Proc Natl Acad Sci U S A *92*, 1739-1743.

Zaychikov, E., Denissova, L., Meier, T., Gotte, M., and Heumann, H. (1997). Influence of Mg2+ and temperature on formation of the transcription bubble. J Biol Chem *272*, 2259-2267.

APPENDIX A:
SUPPLEMENTAL FIGURES

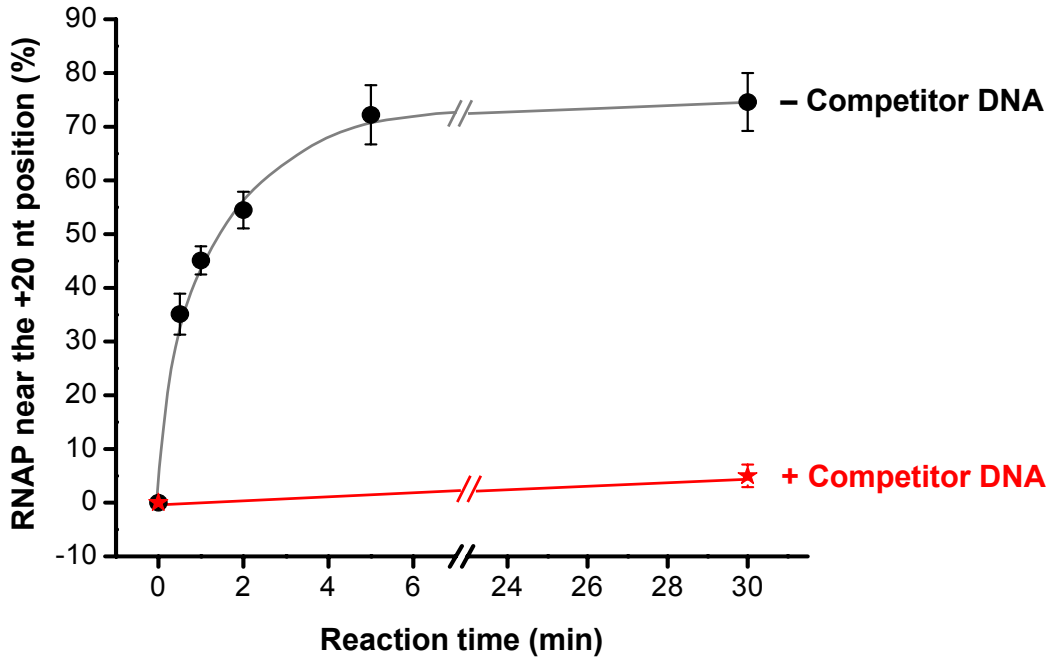

Figure A.1. Competitor DNA Prevents Re-initiation on Nucleosomal Templates

An experiment was conducted to determine how effective competitor DNA was in preventing re-initiation. The competitor DNA was 250 bp in length and contained a single T7A1 promoter. 0.4 nM single promoter template, in the absence or presence of competitor DNA, was mixed with 2 nM RNAP together with 1 mM ApUTP, ATP, GTP, and CTP at concentrations identical to those used in experiments described in the text. This allowed any RNAP that might initiate from the promoter to advance to at most the +20 nt position. Transcription reactions were quenched by the addition of EDTA at given time points and the percentage of DNA that formed a PTC near the +20 nt position

was determined by DNA unzipping. Data are shown as (mean ± s.e.) and smooth curves were drawn for clarity (not fits). In the absence of competitor DNA, a PTC was able to form on the experimental DNA template in ~ 1 min and the percentage formed plateaued at ~ 75% by 30 min. However, in the presence of competitor DNA, only a very small fraction of the experimental DNA templates formed a PTC. Even after 30 min, this fraction was < 5%. Competitor DNA ensured single round transcription in the experiments.

To exclude the possibility that competitor DNA dissociated the RNAP and/or nucleosome from experimental DNA templates, RNAP was first walked to the +20 nt position on nucleosomal DNA templates, and after 30 min incubation in the presence or absence of competitor DNA, the percentage of the RNAP/nucleosome remaining on the DNA template was examined using the unzipping method. The presence of competitor DNA had no detectable effect on the binding or unzipping signatures of the RNAP/nucleosomes (data not shown).

Figure A.2. Heparin Removes Histones without Dissociating RNAP

These experiments were conducted to determine the effectiveness of heparin in removing histones and whether heparin altered the locations of RNAP.

(a) Increasing heparin concentration converted nucleosomes to naked DNA. Heparin has previously been shown to completely or partially remove histones (Bancaud et al., 2007). Here native gel analysis confirmed that increasing heparin concentration converted nucleosomal DNA to naked DNA. This was further confirmed by DNA unzipping assays (data not shown). In all experiments presented in the main text requiring histone dissociation, 4 mg/ml of heparin was used.

(b) Heparin removes histones without dissociating RNAP or altering its unzipping signature. After a PTC was formed on a nucleosomal template, the sample was incubated with heparin at room temperature for 30 min, and the DNA was unzipped. The unzipping data show that heparin only dissociated histones without dissociating the RNAP or altering its location and/or unzipping signature.

a

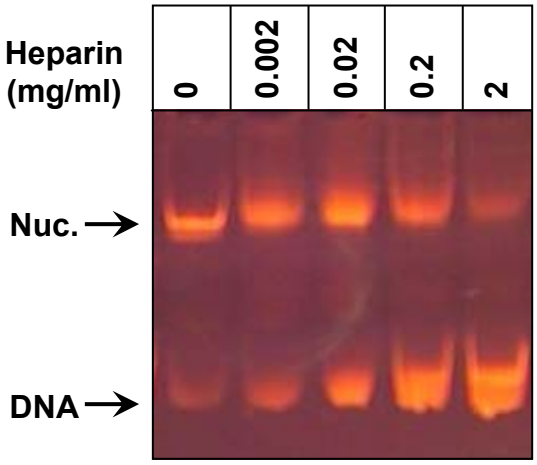
Heparin
(mg/ml)
0
0.002
0.02
0.2
2
Nuc.
DNA

b

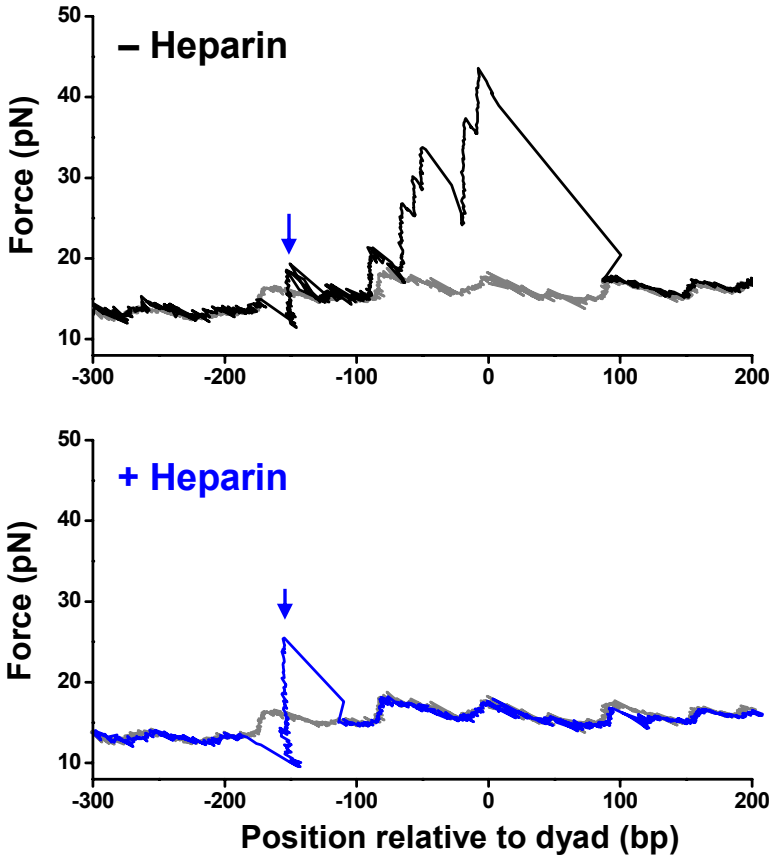
– Heparin
+ Heparin
Force (pN)
50
40
30
20
10
-300
-200
-100
0
100
200
Position relative to dyad (bp)

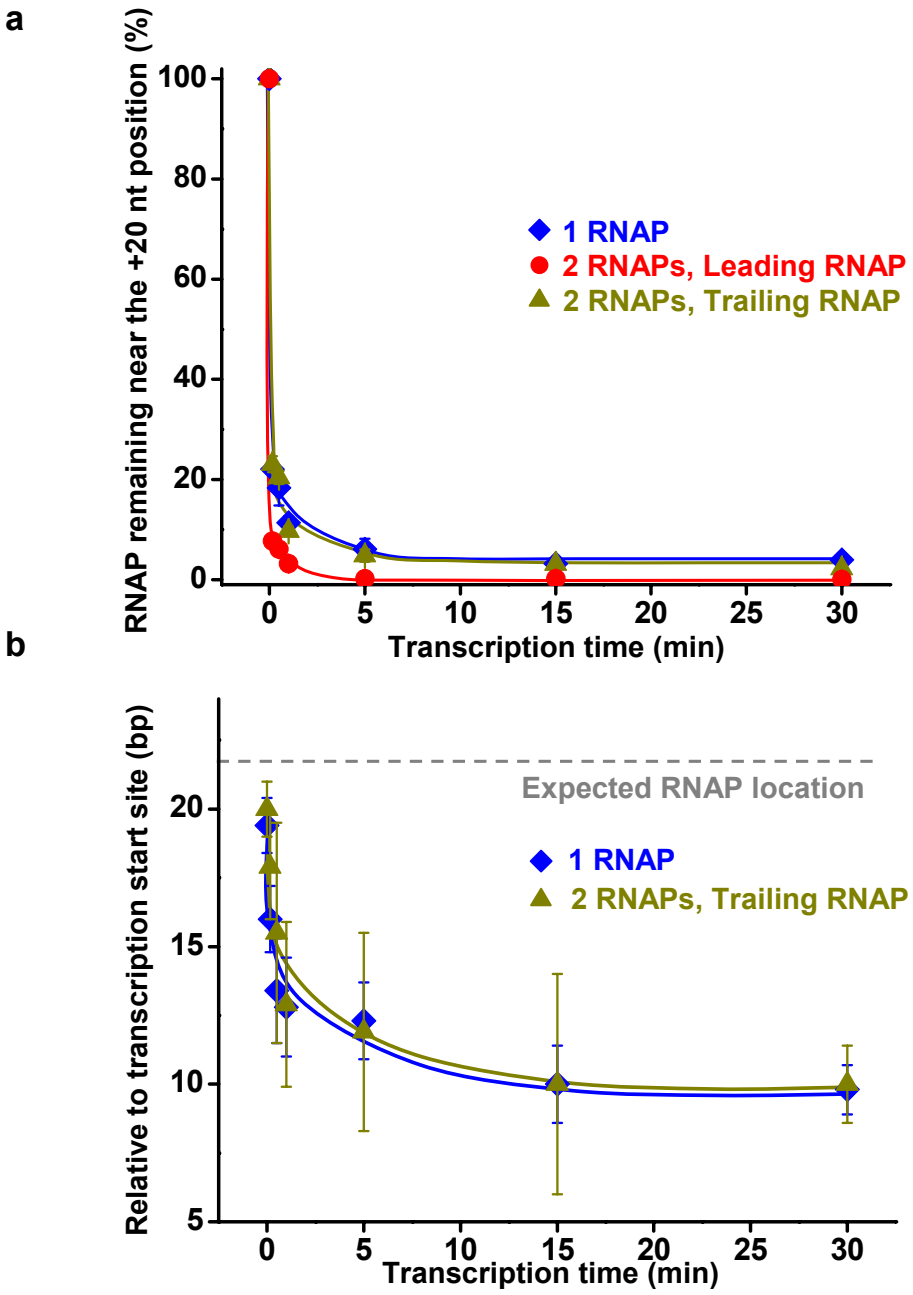

Figure A.3. Location of RNAP on DNA in a PTC

To determine the location of an RNAP on the DNA template when a PTC was formed with an RNA length of +20 nt, we unzipped DNA through the PTC on both the single promoter template (Figure 2.4a) and the two-promoter template (Figure 2.10a) prior to NTP addition and at different time points after NTP addition. EDTA was used to quench the reaction before single molecule data were taken. Only RNAP detected near the +20 nt position were examined in order to reveal the time course of escape from the stalled state. Data points are represented as (mean ± s.e.). The smooth curves were drawn for clarity (not fits).

(a) Percentages of RNAP remaining near the +20 nt position on the single-promoter template and the two-promoter template were plotted as a function of transcription time (also see Figure 4C for two-promoter template case). The majority of the RNAP resumed transcription immediately (< 10 s, the shortest measurement time) after 1 mM NTP was added. Only < 5% of the RNAP remained near + 20 nt after 5 min in all cases.

(Bb The location of RNAP remaining vs. transcription time. Before NTP addition, the mean location of the force rise was found to be ~ 3 bp upstream of the expected location (grey dashed line at +22 bp). As the transcription time increased, the fraction remaining near + 20 nt decreased, and the mean location of the remaining RNAPs shifted upstream away from the expected location for both RNAPs on the single promoter template and trailing RNAPs on the two-promoter template. This indicates that more extensively backtracked RNAPs took longer to exit a backtracked state.

APPENDIX B:
SUPPLEMENTAL DISCUSSION

Calculation of Runoff Efficiencies

In order to calculate the runoff efficiency shown in Figure 2.12, we needed to correct for two small but significant contributions: templates without a nucleosome at the 601 NPE or without the formation of a PTC. Using the DNA unzipping method, we determined conditions under which the probability of PTC formation at a promoter (P_{RNAP}) was at least 90% and the probability of a template containing a nucleosome (P_{nuc}) was also at least 90%.

For the single-promoter template, at a given transcription time, if the measured probability of a template being naked was $P_{0,\mathrm{raw}}^{1\mathrm{RNAP}}$, then the corrected runoff efficiency was calculated as.

$$P_0^{1\mathrm{RNAP}} = \frac{P_{0,\mathrm{raw}}^{1\mathrm{RNAP}} - \left(1 - P_{\mathrm{RNAP}} P_{\mathrm{nuc}}\right)}{P_{\mathrm{RNAP}} P_{\mathrm{nuc}}}$$

For the two-promoter template, at a given transcription time, if the measured probability of a template being naked was P_0, containing a single RNAP P_1, and containing two RNAPs P_2, then the corrected runoff efficiency of the leading RNAP was calculated as,

$$P_0^{\mathrm{leading}} = 1 - \frac{P_2}{P_{\mathrm{RNAP}}^2 P_{\mathrm{nuc}}}$$

and of the trailing RNAP:

$$P_0^{\mathrm{trailing}} = \frac{P_0 - (1 - P_{\mathrm{nuc}}) - 2P_{\mathrm{RNAP}} P_{\mathrm{nuc}} (1 - P_{\mathrm{RNAP}}) P_0^{1\mathrm{RNAP}}}{P_{\mathrm{RNAP}}^2 P_{\mathrm{nuc}}}$$

APPENDIX C:
EXPERIMENTAL PROCEDURES

Nucleosomal DNA Templates for Transcription

We prepared nucleosomal DNA templates using methods similar to those previously described (Koch et al., 2002; Shundrovsky et al., 2006; Hall et al., 2009), except that these templates contained either one or two promoters. Briefly, each DNA construct consisted of an anchoring and an unzipping segment (Figure 2.1a). An ~1.3 kbp anchoring segment was labeled by digoxigenin at one end and a ligatable *DraIII* overhang at the other end. Two unzipping segments were constructed. The single-promoter segment was 792 bp long and composed of one T7A1 promoter followed by one 601 NPE (Figure 2.4a). The two-promoter segment was 850 bp long and contained two T7A1 promoters 162 bp apart, followed by a 601 NPE (Figure 2.10a). Both segments were synthesized by PCR using a biotin-labeled primer. The PCR products were then digested by restriction enzyme *DraIII* to generate a ligatable end and dephosphorylated using CIP (NEB) to introduce a nick into the final DNA templates. Nucleosomes were assembled onto the unzipping segments using purified HeLa histones by a well established salt dialysis method. The anchoring and unzipping segments were joined by ligation immediately prior to use. This produced a complete template that was labeled with a single dig tag on one end and a biotin tag located 5 bp away from the nick in one DNA strand.

Transcription Assays

Bulk transcription assays: Transcription was first initiated by incubation of 20 nM *E. coli* RNAP, 4 nM transcription DNA template, 250 μM ApU initiating

dinucleotide, 50 μM ATP/GTP, and α-[^{32}P] CTP [5 μCi (1 μCi = 37 GBq) at 3,000 Ci/mmol] in transcription buffer (TB: 25 mM Tris•Cl, pH 8.0, 100 mM KCl, 4 mM $MgCl_2$, 1 mM DTT, 3% (v/v) glycerol, 0.15 mg/mL acetylated BSA) for 20 min at 37ºC to form PTCs which contained DNA, RNAP and 20 nt RNA transcript. PTCs were then diluted 10 fold in TB and transcription was resumed at room temperature (23ºC ± 1ºC) by addition of 1 mM of all four unlabeled NTPs. To prevent re-initiation, competitor DNA was added to 15 nM to serve as an RNAP sink immediately before the resumption of transcription (Figure A.1). Transcription reactions were quenched at predetermined time points by addition of EDTA to 10 mM. Transcripts were analyzed on polyacrylamide sequencing gels and imaged with PhosphorImager (Molecular Dynamics) (Shundrovsky et al., 2004).

Single molecule transcription assays: Transcription reactions were typically performed using identical protocols as in bulk transcription assays except that 50 μM unlabeled CTP was used instead of α-[^{32}P] CTP during PTC formation. After the transcription reactions were quenched, 4 mg/ml heparin was used to chemically dissociate histone proteins. Single molecule sample preparation was then immediately performed using protocols similar to those previously described (Koch et al., 2002). In the experiments where RNase T1 was needed, 5 units/μl was added right before the addition of NTPs. For experiments described in Figure 1B, PTCs at +20 nt were formed by incubating 2 nM RNAP, 0.4 nM DNA template, and 1mM ApUTP and ATP/GTP/CTP in transcription buffer for 2 min at room temperature before the reaction was quenched by EDTA.

Single Molecule DNA Unzipping Experiments

The experimental configuration for optical trapping was similar to that previously described (Figure 2.1b) (Koch et al., 2002). Briefly, one end of an anchoring segment was attached to a microscope coverslip via a digoxigenin/anti-digoxigenin connection. The 5' nicked unzipping segment was attached to a 0.48 μm-diameter microsphere via a biotin-strepavidin connection. A single-molecule optical trapping setup was used to unzip the DNA template by moving the coverslip horizontally away from the optical trap. When a bound protein was encountered, a computer-controlled feedback loop increased the applied load linearly with time (8 pN/s) as necessary to unzip through the protein-DNA interactions. Data were digitized at 12 kHz and boxcar-averaged to 60 Hz. The acquired data signals were converted into force and number of base pairs unzipped as described. Additionally, the force-versus-base pair unzipped curves were aligned as previously described to achieve high precision position detection (Hall et al., 2009).